

2  
AEDC-TR-68-139

**ARCHIVE COPY  
DO NOT LOAN**

*cy*



## **INITIAL RESULTS FROM A COMBINED SPACE ENVIRONMENT EFFECTS CHAMBER**

**W. G. Kirby and C. N. Warren**

**ARO, Inc.**

**October 1968**

This document has been approved for public release  
and sale; its distribution is unlimited.

**AEROSPACE ENVIRONMENTAL FACILITY  
ARNOLD ENGINEERING DEVELOPMENT CENTER  
AIR FORCE SYSTEMS COMMAND  
ARNOLD AIR FORCE STATION, TENNESSEE**

AEDC TECHNICAL LIBRARY



PROPERTY OF U. S. AIR FORCE

AEDC LIBRARY

F40600 - 69 - C - 0001

# ***NOTICES***

When U. S. Government drawings specifications, or other data are used for any purpose other than a definitely related Government procurement operation, the Government thereby incurs no responsibility nor any obligation whatsoever, and the fact that the Government may have formulated, furnished, or in any way supplied the said drawings, specifications, or other data, is not to be regarded by implication or otherwise, or in any manner licensing the holder or any other person or corporation, or conveying any rights or permission to manufacture, use, or sell any patented invention that may in any way be related thereto.

Qualified users may obtain copies of this report from the Defense Documentation Center.

References to named commercial products in this report are not to be considered in any sense as an endorsement of the product by the United States Air Force or the Government.

# ERRATA

AEDC-TR-68-139, October 1968

## INITIAL RESULTS FROM A COMBINED SPACE ENVIRONMENT EFFECTS CHAMBER

W. G. Kirby and C. N. Warren, ARO, Inc.

Arnold Engineering Development Center  
Air Force Systems Command  
Arnold Air Force Station, Tennessee

The symbol identification on Figs. 13 and 14 (pages 38 and 39) should appear as shown below.

Fig. 13    □    Before Irradiation  
            ○    After Irradiation  
            △    After 21-hr Exposure to O<sub>2</sub>  
            ◇    After 220-hr Exposure to Air

Fig. 14    ○    Before Irradiation  
            △    After Irradiation  
            □    After 21-hr Exposure to O<sub>2</sub>  
            ◇    After 220-hr Exposure to Air

This document has been approved for public release and sale; its distribution is unlimited.
--

INITIAL RESULTS FROM A COMBINED SPACE  
ENVIRONMENT EFFECTS CHAMBER

W. G. Kirby and C. N. Warren  
ARO, Inc.

This document has been approved for public release  
and sale; its distribution is unlimited.

## FOREWORD

The research presented in this report was sponsored by the Arnold Engineering Development Center (AEDC), Air Force Systems Command (AFSC), Arnold Air Force Station, Tennessee, under Program Element 6540223F.

The results presented were obtained by ARO, Inc. (a subsidiary of Sverdrup & Parcel and Associates, Inc.), contract operator of the AEDC, AFSC, under Contract F40600-69-C-0001. The research was conducted under ARO Project No. SW3801, and the manuscript was submitted for publication on June 5, 1968.

This technical report has been reviewed and is approved.

Ward F. Petrie  
Captain, USAF  
Advanced Plans Division  
Directorate of Plans  
and Technology

Edward R. Feicht  
Colonel, USAF  
Director of Plans  
and Technology

## ABSTRACT

A combined environment research chamber has been designed and built to provide the capability of irradiating test samples with protons, electrons, and electromagnetic radiation, individually, sequentially, or simultaneously, in a clean high vacuum utilizing a multisample holder and an in situ spectral reflectance measurement technique. The chamber performance was evaluated on the basis of a combined environment test conducted on a titanium dioxide-methyl silicone thermal control coating and was found to be completely satisfactory. In the combined environment experiment, samples of the thermal control coating were exposed individually to vacuum, protons, electrons, electromagnetic radiation, and to all of these constituents simultaneously. No synergistic effects were noted. However, a combined environment interaction was noted wherein the sum of the individual effects was greater than that obtained in the simultaneous exposure. Electron irradiations were carried out at rates that were different by an order of magnitude, and a measurable difference was obtained for the same time integrated flux. It is suggested that the electron rate effect is a possible cause of the observed combined environment interaction. Observations during the experimental runs indicated considerable outgassing, arcing, and glow discharge during the electron irradiation. Microscopic examination revealed surface roughening and cracking, and an amber discoloration of proton irradiated samples. Infrared reflectance measurements on irradiated samples did not give a positive indication of structure change within the methyl silicone binder.

## CONTENTS

	<u>Page</u>
ABSTRACT . . . . .	iii
I. INTRODUCTION . . . . .	1
II. EXPERIMENTAL APPARATUS	
2.1 Test Chamber. . . . .	3
2.2 Test Sample . . . . .	3
2.3 Sample Holder . . . . .	4
2.4 Spectral Reflectance System . . . . .	4
2.5 Radiation Injection System . . . . .	6
2.6 Special Instrumentation . . . . .	9
III. PROCEDURE . . . . .	9
IV. RESULTS AND DISCUSSION	
4.1 Combined Environment Effects . . . . .	10
4.2 Rate Effects . . . . .	15
4.3 Bleaching . . . . .	17
4.4 Structure Examination . . . . .	18
4.5 Microscopic Examination. . . . .	18
V. CONCLUDING REMARKS. . . . .	20
REFERENCES. . . . .	21

## APPENDIXES

## I. ILLUSTRATIONS

Figure

1. Schematic of the Combined Environment Test Chamber . . . . .	25
2. Combined Environment Chamber . . . . .	26
3. Combined Environment Sample Holder . . . . .	28
4. Carbon and Mercury Arc Lamps . . . . .	29
5. Proton and Electron Accelerator . . . . .	30
6. Spectral Irradiance of the Electromagnetic Test System and the Sun . . . . .	31
7. Optical Degradation of TiO <sub>2</sub> -Methyl Silicone Thermal Control Coating from Electromagnetic Radiation . . . . .	32
8. Optical Degradation of TiO <sub>2</sub> -Methyl Silicone Thermal Control Coating from Electron Irradiation . . . . .	33
9. Optical Degradation of TiO <sub>2</sub> -Methyl Silicone Thermal Coating from Proton Irradiation . . . . .	34

<u>Figure</u>	<u>Page</u>
10. Optical Degradation of TiO <sub>2</sub> -Methyl Silicone Thermal Control Coating from Simultaneous Electron, Proton, and Electromagnetic Irradiation . . . . .	35
11. Integrated Solar Absorption versus Irradiation . . . . .	36
12. Recovery of Combined Environment Irradiated TiO <sub>2</sub> -Methyl Silicone Thermal Control Coating upon Exposure to O <sub>2</sub> . . . . .	37
13. Recovery of Proton Irradiated TiO <sub>2</sub> -Methyl Silicone Thermal Control Coating upon Exposure to O <sub>2</sub> . . . . .	38
14. Recovery of Electron Irradiated TiO <sub>2</sub> -Methyl Silicone Thermal Control Coating upon Exposure to O <sub>2</sub> . . . . .	39
15. Recovery of Electromagnetic Irradiated TiO <sub>2</sub> -Methyl Silicone Thermal Control Coating upon Exposure to O <sub>2</sub> . . . . .	40
16. Infrared Spectra of a Nonirradiated Sample. . . . .	41
17. Infrared Spectra of Electron Irradiated (Low Rate) Sample. . . . .	42
18. Infrared Spectra of Proton Irradiated Sample. . . . .	43
19. Infrared Spectra of Electron Irradiated (High Rate) Sample. . . . .	44
20. Infrared Spectra of Electromagnetic Radiation Sample. . . . .	45
21. Infrared Spectra of Combined Environment Sample . . . . .	46
22. Photomicrograph of the Surface of the Test Samples. . . . .	47
23. Photomicrograph of the Cross Section of the Test Samples . . . . .	48

## II. TABLES

I. Combined Environment Effects Evaluation as Determined by Changes in the Spectral Reflectance of Coating . . . . .	49
II. Combined Environment Effects Evaluation as Determined by Integrated Solar Reflectance and Absorptance . . . . .	50
III. Electron Rate Effect Summary . . . . .	51

## SECTION I

### INTRODUCTION

A significant research and development effort has been expended to provide ground test capabilities in support of near-earth manned space flights. Vacuum-thermal simulation in ground facilities was the basic requirement for these missions. Most of the present large space simulation facilities have approximated this test environment. However, as space flights become more complex and lengthy, a more complete space environment simulation is required for ground checkout of these vehicles.

The charged particle constituent of the space environment appears to be a logical next step in ground simulation. These particles surround the earth in the auroral and trapping regions, and are found farther out in space in the solar wind, solar cosmic rays (solar flares), and galactic cosmic rays. It is also possible that trapped radiation belts exist around other planets similar to those discovered around the earth.

Unmanned space probes have shown that this constituent of the space environment is severe and warrants study in ground test facilities (Ref. 1). Initial experimental work in this area has indicated that there are problems that should be investigated in order to ensure agreement between ground results and space flight data. In some cases these laboratory experiments have indicated that the sum of the effects obtained by individual exposure of space materials to the constituents of the space environment is less than that obtained by simultaneous exposure to the complete or combined environment. This interaction between the constituents of the environment has been referred to as a "synergistic effect" (Refs. 2 through 5). The evaluation of this problem is necessary for planning future space environmental facilities and the extrapolation of test results to flight hardware. Much consideration has also been given to accelerated testing in order to produce more timely results from such facilities. This refers to the use of environmental exposure rates that are much higher than those in space. Results are becoming available that point out the fallacy of excessive exposure rates since this can produce effects that are not representative with space flight data (Ref. 6). In a similar way the method by which the environmental effects are measured has a tremendous influence on the validity of the data. A change in environment for test damage measurement has produced misleading results (Refs. 7 and 8). The utilization of in situ measuring techniques and the evaluation of rate and synergistic effects are essential for the production of timely and accurate data in new and improved space environmental test facilities. The importance of reproducing the solar radiation spectrum has not been evaluated; however,

there is some indication (Ref. 6) that this may become important as more data are accumulated.

This report describes the combined environment research chamber that has been developed to investigate these problem areas. Initial test results on a thermal control material,\* composed of titanium dioxide ( $\text{TiO}_2$ ) in a methyl silicone binder, are presented to evaluate (1) the performance of the system, (2) the irradiation rate effect, and (3) the combined environment interaction, or the so-called synergistic effect.

## SECTION II EXPERIMENTAL APPARATUS

The combined environment test chamber (Fig. 1, Appendix I) described in this report is intended for general use in the development of combined environment testing techniques. The purpose of the initial investigation was to evaluate the chamber performance and its adequacy to determine the dependence of the change in spectral reflectance of a thermal control coating on irradiation rate and the sample environment. The initial samples were magnesium disks covered with a thermal control coating composed of a titanium dioxide pigment in a methyl silicone binder. There are certain objectives that must be attained by this experimental system for this and subsequent investigations. The design of this system has been governed by the following considerations:

1. A noncontaminating environment must be maintained within the test chamber for the duration of the experiment to avoid interaction between (1) the incident radiation and contaminants on the sample surface, and (2) the irradiated sample and contaminants.
2. Spectral reflectance measurements should be made in situ in order to avoid the possibility of contaminating or bleaching the samples.
3. Operational test pressures in the  $10^{-8}$  to  $10^{-11}$  torr range must be available.
4. Flexibility must be provided in the radiation injection system so that samples may be irradiated individually, sequentially, or simultaneously by all sources of radiation.

---

\*Supplied through the courtesy of the Lockheed Missiles and Space Company, Palo Alto, California.

5. Provisions must be made for the isolation of the radiation injection system from the test chamber such that a malfunction in this system would not jeopardize the test samples.
6. In order to reduce gas loads from sources external to the main chamber, pumping systems must be placed as close as possible to the source of these loads and before every opening into the chamber. The flow conductance from the source to the chamber must be kept as small as practical.
7. A multisample holder sufficient to complete a given phase of testing is desirable in order to minimize time-consuming excursions between testing and atmospheric conditions.
8. Clean pumping systems must be employed at all locations within the system.

The resulting apparatus is described in the following sections.

## 2.1 TEST CHAMBER

The test chamber is a vertical, cylindrical, ultrahigh vacuum chamber of stainless steel construction, 24 in. in diameter and 68.5 in. in length (Figs. 2a and b). The chamber is flanged 32.5 in. from the bottom. The bottom section of the chamber contains a 400 liters/sec ion pump and a titanium sublimation pump. This section has a combined pumping speed for air in excess of 6000 liters/sec. The titanium sublimation surface is liquid-nitrogen (LN<sub>2</sub>)-cooled. Just below the flange of this section and spaced evenly around the circumference of the chamber are twelve 1.5-in. -diam instrumentation ports. The top of the chamber is removable and contains two 4-in. ports and one 8-in. port spaced 90 deg apart around the circumference of the midpoint of this section.

The chamber is evacuated by an LN<sub>2</sub> trapped mechanical pump through an isolation valve in the bottom section of the chamber. The ion pump is turned on after the chamber has been evacuated to a pressure sufficiently low to prevent glow discharge, and then the isolation valve is closed. Titanium sublimation pumping is used as needed. The empty chamber as described has an ultimate pressure below  $5 \times 10^{-11}$  torr as measured by a trigger-type cold cathode gage.

## 2.2 TEST SAMPLE

The test material is a titanium dioxide-methyl silicone thermal control coating produced by Dow Corning as No. 92-007 aerospace

sealant. The substrate for the thermal control coating was a 1.25-in. -diam magnesium disk, approximately 0.050 in. thick, coated with Dow Corning A-4094 silicone rubber primer. The coating thickness on these samples was approximately 0.004 in. thick. Five of these samples were mounted in the sample holder as described in the following section.

### 2.3 SAMPLE HOLDER

The sample holder (Fig. 3) is a horizontal 18-in. -diam aluminum plate 0.5 in. thick. The holder is suspended from the top of the chamber by a stainless steel rod that is welded to a high vacuum rotary feedthrough and positioned by two nylon bearings. The rotary feedthrough vacuum seal is made through a stainless steel bellows to a chamber flange. The feedthrough is mounted on a movable table that provides translation, vertical, and angular motion to the mounting rod. The holder is screwed onto the mounting rod and clamped in place by two knurled nuts and lock washers in order to provide additional vertical alignment.

Right-angle aluminum sample and sensor mounts are spaced evenly around the circumference of the holder. A total of 25 mounts can be accommodated on the holder. The centers of the samples or sensors are located on a plane formed by the centers of the three ports that are used for irradiation, viewing, and reflectance measurements. There are indexing marks along the circumference of the holder such that the alignment of an indexing mark and pointer at the viewing port positions the samples at either the irradiation or reflectance measuring position. The sensors are indexed so they may be positioned at the irradiation position. The sensors include Faraday cups for beam profile and intensity measurements, a quartz disk for beam viewing, and a detector for electromagnetic radiation intensity.

Reflectance measurements are facilitated by the contact points for the flat external side of the integrating sphere that is utilized to measure the reflectance of the samples. The points are located 120 deg apart around the edge of a 1.25-in. -diam sample. The integrating sphere, when touching all three points, is approximately 0.001 in. away from the sample surface. The position of the integrating sphere on the points is indicated electrically by an external meter.

### 2.4 SPECTRAL REFLECTANCE SYSTEM

The spectral reflectance system consists of (1) the integrating sphere, detectors, and traversing device inside the vacuum chamber;

(2) a monochromator and transfer optic from the monochromator to the integrating sphere; and (3) the detector signal preamplifier, amplifier, and readout, and a light-beam chopper.

The external shape of the integrating sphere is in the form of a cube in order to facilitate mounting of the detectors and the sphere. The centers of the detector ports and the sample port on the 2-in. -diam sphere are on the same plane and are located 90 deg apart on a circle within this plane. The detector ports are opposite each other. The light entrance port is opposite the sample port, but it is positioned off the plane of the centers of the other ports so that light will always strike the sample at a small angle. A lead sulfide and an IP28 photo-multiplier tube detector are mounted externally on the sphere. The sphere is supported by a metal stirrup that is attached to a translational high vacuum feedthrough located above a 4-in. port. The feedthrough is actuated by an external manual drive.

The internal configuration of the integrating sphere is quite important for these tests. In a classical sphere (Ref. 9) the spectral reflectance of a sample is obtained from the following relation:

$$R_s = R_w \frac{D_s}{D_w} \quad (1)$$

where  $R_w$  is the reflectance of the wall coating,  $D_w$  is the detector output when monochromatic light initially shines on the sphere wall, and  $D_s$  is the detector output when the light initially shines on the sample. In this case the absolute reflectance of the sample can be obtained only if the spectral reflectance of the wall material is known and if it remains stable over prolonged periods in a vacuum. In order to avoid the stability problem, two elliptical shields coated with magnesium oxide were inserted within the sphere such that first reflection from the sample would not be seen by either detector. Equation (1), with this change in geometry, becomes the following expression (Ref. 10):

$$R_s = \frac{D_s}{D_w} \quad (2)$$

The spectral reflectance, as determined by this relationship, is independent of changes in the reflectance of the sphere wall coating as long as these changes occur uniformly over this surface. The mechanical stability of the magnesium oxide wall coating has been excellent during these tests.

Monochromatic light is produced for these measurements by a properly filtered grating monochromator. The light beam is interrupted

by a chopper. The pulsed light beam is transmitted to the sphere by means of a two-position flip mirror, two focusing mirrors, and two quartz chamber windows (Fig. 2a). The detector signal is relayed to a recorder by a preamplifier and synchronous amplifier.

## 2.5 RADIATION INJECTION SYSTEM

This system provides a means of introducing any combination of three types of radiation into the main test chamber with a minimum of additional gas load. It may be isolated from the main test chamber and serve as an independent checkout chamber for the radiation sources.

The basic part of this system is an antechamber attached through a 4-in. isolation valve to the 8-in. port on the main chamber. The antechamber is a 12- by 12-in. stainless steel cylinder with four 4-in. -diam ports spaced 90 deg apart around the circumference at the mid-point of the chamber. One of these ports is connected through a 6-in. isolation valve to a titanium sublimation and ion pumping unit. This pumping system produces the vacuum for this section when used independently of the main chamber, and when used in conjunction with the main chamber it provides pumping before the radiation inlet orifices into the main chamber in order to reduce the gas load. A second port serves as a vacuum electrical feedthrough for an electron and proton pickoff grid mounted in the path of these beams in the antechamber. These grids are used to monitor the beams when irradiating a sample. The other two ports are for viewing and utilize lead glass windows.

In the center of the rear surface of this section are five 1.5-in. -OD tubes in order to provide a means for radiation to enter the antechamber and to provide a shutter for the radiation beams. Four of these tubes are spaced 90 deg apart on a 6-in. -diam circle at an angle of 5 deg to the normal of this surface. The fifth tube is normal to the surface at the center of this circle. The top and bottom tubes are evacuated and connected respectively to the proton and electron accelerator. A titanium sublimation and ion pump is located at the exit of the proton accelerator in order to remove gas originating in the accelerator. The two side tubes are approximately 10 in. long and terminate with a quartz window. One of these tubes transmits the radiation from a mercury arc lamp and the other transmits the radiation from a carbon arc. The remaining tube is terminated with a vacuum rotary feedthrough in order to externally operate a shutter for the beams with respect to the sample or instrumentation. A 1-in. orifice for each beam is provided at the exit of the antechamber.

### 2.5.1 Electromagnetic Radiation

The electromagnetic radiation for these experiments was obtained by combining the output from two sources at the sample. These sources were a carbon arc and a mercury arc lamp.

The mercury arc lamp (Fig. 4 and Ref. 11) is an air-cooled, high-pressure source. Transfer optics transmit the radiation and provide a means to vary the intensity at the sample. The purpose of this lamp is to supplement the ultraviolet spectrum of the carbon arc lamp.

In the carbon arc lamp (Fig. 5 and Ref. 12) the carbon rods are advanced by an automatic drive and are consumed at the rate of one rod every 40 min. External optics provide a variable intensity at the sample.

At the present it is realized that there is not an adequate method for reproducing the spectral irradiance of the sun. The spectral irradiance achieved by this lamp system is illustrated by a comparison of the spectral irradiance of this system at the sample to that of the sun (Ref. 13) as shown in Fig. 6. The total intensity of this system for these experiments was 0.68 solar constant.

### 2.5.2 Electron Accelerator

The electron accelerator (Fig. 5) is composed of a hot tungsten filament as a source of electrons, a bias cup, and an accelerating tube. These elements are mounted in a 5.5-in. -OD by 15-in. -long cylindrical stainless steel housing such that the external side of these elements is exposed to an insulating atmosphere of sulfurhexafluoride. The internal side of these elements was sealed by O-rings from 5 atm of the insulating gas and was connected by an external flange with tubing to the rear of the radiation injection system.

The accelerator tube is composed of alternate sections of glass (2-in. -OD) and stainless steel (2.5-in. -OD). The diameter of the beam passage through this section is 0.825 in. The accelerating potential is distributed evenly across the tube by means of a resistive spiral coating painted on each glass section. The accelerating voltage, filament current, and bias voltage are supplied by a combined power supply. This supply produces from 0 to 350 kv dc accelerating voltage at a rated current of 1 ma and for the filament and bias supply, respectively, 100 v-amp insulated for 350 kv dc.

The power supply is located behind a high voltage barricade, and the output required by the accelerator is transmitted by high voltage cable.

The accelerator is operated remotely from a control panel (Fig. 2a) near the test chamber.

### 2.5.3 Proton Accelerator

The proton accelerator (Fig. 5) consists of the following units: (1) power supply, (2) high voltage deck, (3) ion source, and (4) the accelerating tube.

The power for operating the accelerator is supplied from two units: (1) a high voltage, low current supply, and (2) a low voltage supply insulated against a high voltage. The operating range of the high voltage supply is from 0 to 130 kv dc with a maximum current of 2 ma. The output from this source is transmitted by high voltage cable to the top of the high voltage deck. An isolation transformer provides 110 v ac, 3 kva service for the ion source at the top of the high voltage deck by means of a high voltage cable. This transformer provides insulation for 150 kv dc. These supplies are located within the high voltage barricade and are operated from a central control station.

The high voltage deck assembly is 28 in. wide by 48 in. long and approximately 63 in. high. The aluminum dome, which is used to cover the ion source electronics, adds another 19 in. to the height of the assembly. The assembly is composed of aluminum plates (28 by 48 in.) supported and spaced by phenolic rods. The spacing between these plates is 4.375 in. with the exception of the top plate which has a spacing of 6.25 in. The deck is mounted to a base of channel aluminum for ease in transporting this assembly. The main support of the deck is accomplished by four solid 3-in. -OD phenolic rods. The spacing of the plates was maintained by cutting and inserting the appropriate length of 3-in. -ID phenolic tubing. Aluminum tubing was welded to the edge of the plates to serve as corona rods. Each plate was connected electrically to the adjoining plate by a resistor. The top and bottom plates were connected, respectively, to the high voltage power supply and to ground. This produced a uniform potential gradient from the top to the bottom of the assembly that was applied to the accelerating tube by means of copper tubing connectors from each plate. The ion source and the front end of the accelerator tube are mounted on the top of the deck transformer. Openings are provided in the dome for the accelerating tube and for the ion source phenolic control rods that extend over to the main control area.

The ion source system consists of an RF ion source, lens, and a palladium leak. All of these items are located on top of the high voltage deck and are operated by remote control. Pure hydrogen gas is supplied

to the glass plasma bottle through the palladium leak. A hydrogen plasma is created in the bottle by the field of an 80-MHz oscillator. An extraction voltage applied across the bottle removes ions from the plasma. Specification for the ion source provides that for a maximum extraction voltage of 5000 v a current of at least 1 ma will be obtained with a minimum  $H^+$  ion (protons) concentration of 85 percent with the remainder being  $H_2^+$  or neutral hydrogen. The ion source output is focused by the lens.

The accelerator tube is approximately 25.5 in. long. The tube is composed of alternate glass and metal sections. The metal sections externally provide a means of attaching the copper tubing leads from the high voltage potential divider to the accelerating tube. Internally the metal sections shield the beam so that it is affected only by the accelerating potential applied to each metal section. The minimum internal opening for the beam is 4 in. The external dimensions of the glass and metal sections are, respectively, 7 and 7.75 in. The lower end of the tube is at ground potential, and is connected to a 1.5-in. evacuated tube that goes into the rear of the radiation injection system.

## 2.6 SPECIAL INSTRUMENTATION

The gas pressure and composition within the test chamber were monitored, respectively, by a trigger high vacuum gage and a residual gas analyzer. An X-Y plotter recorded the output of the residual gas analyzer. All electron and proton beam Faraday cup outputs were measured by a micromicroammeter.

## SECTION III PROCEDURE

The main test chamber was evacuated to below  $5 \times 10^{-9}$  torr, and the background gas content was monitored by a mass spectrometer until the oxygen partial pressure was negligible. A pressure of  $5 \times 10^{-9}$  torr was postulated as the maximum allowable test pressure for these initial experiments.

The radiation injection system pressure was reduced to  $1 \times 10^{-8}$  torr. The isolation valve between the main chamber and the radiation injection system was opened after this pressure was attained, and the chamber background gas was monitored at intervals while this valve remained open.

The radiation beams required for a particular experiment were activated and allowed to impinge on the quartz viewing disk on the sample holder. The outline of the sample on the disk is such that a beam impinging on this outline would hit the sample in precisely the same manner when it is in turn rotated into position. Each beam was focused and the intensity was set. The monitoring grid currents for the particle beams were recorded along with the detector reading for the electromagnetic beam. The isolation valve was closed with test beams on, and the sample to be irradiated was rotated into position. Then the isolation valve was opened simultaneously with the activation of the irradiation timer. After a desired time of radiation, the isolation valve was closed and in situ spectral reflectance measurements were made on the sample. This same procedure was followed until the desired total irradiation time was achieved for each sample under the prescribed experimental conditions.

## SECTION IV

### RESULTS AND DISCUSSION

#### 4.1 COMBINED ENVIRONMENT EFFECTS

Other workers (Refs. 2 through 7, see Section I) in this field have indicated the existence of interactions between the constituents of a combined environment. The effect of this interaction has been to produce results from combined environment testing that are much greater than those obtained by summing up the effects from tests made with the individual constituent of the environment under comparable conditions. The enhancement of the test results by this interaction has been commonly referred to as a synergistic effect. In this study a thermal control coating (Section 2.2) was selected to evaluate this and other possible effects. The spectral reflectance of this material was measured to indicate the existence of these effects since this is the principal property governing its use as a thermal control coating. The test coatings were exposed individually and simultaneously to the constituents of the environment, and the change in spectral reflectance was monitored as a function of exposure time. Results were evaluated at an exposure time of 0.717 hr. For these experiments the electron and proton energy and intensity were maintained, respectively, at 50 kev and  $6.3 \times 10^{11}$  particles/cm<sup>2</sup>/sec. The electromagnetic radiation intensity was 0.68 solar constants, and the spectral irradiance was as shown in Fig. 6. The test vacuum, when possible, was maintained below  $5 \times 10^{-9}$  torr.

In Fig. 8 the spectral reflectance of the sample is shown as a function of wavelength for various irradiation times. The degradation of the reflectance was quite severe throughout the spectrum; however, the maximum degradation occurred near the midpoint of the wavelength spectrum.

#### 4.1.4 Proton Irradiation

In the proton irradiation a time of 1.434 hr ( $3.2 \times 10^{15}$  protons/cm<sup>2</sup>) was accumulated on the sample with an energy of 50 kev and an intensity of  $6.3 \times 10^{11}$  protons/cm<sup>2</sup>/sec. The sample temperature remained between 65 and 70°F during this experiment. The pressure in the test chamber was maintained between  $1.0 \times 10^{-9}$  and  $4.5 \times 10^{-9}$  torr for the majority of the irradiation time. A small rise above this pressure range was observed near the midpoint of the irradiation period. The residual gas analyzer indicated a slowly increasing concentration at mass numbers 2 and 16. This is similar to the condition that existed with electron irradiation except that it occurred at a much slower rate. This outgassing probably resulted from the breakdown of the silicone binder.

The local arcing and glow discharge were not observed in this run as they were in the electron irradiation. However, an amber discoloration of the sample was noted after about 15 min of irradiation time. This discoloration is characteristic of proton irradiation and does not appear with any other type of irradiation.

In Fig. 9 the spectral reflectance of the sample is shown as a function of wavelength for various irradiation times. The degradation in reflectance decreased with increasing wavelength. For comparable irradiation times the degradation from the protons was much less than that from the electrons.

#### 4.1.5 Combined Environment Exposure

In the combined environment test the sample was exposed simultaneously to vacuum, electromagnetic radiation, electrons, and protons at the same energy and intensity that was used in the individual irradiation experiments. A total irradiation time of 0.717 hr was achieved with this combined environment. The temperature of the sample was subject to ambient variation and remained in the 62 to 68°F range. The pressure was maintained between  $2.0 \times 10^{-9}$  and  $8.8 \times 10^{-9}$  torr except for a brief rise during the initial 5 min of irradiation. This rise was similar to that obtained in the electron and proton irradiation, and undoubtedly it can be attributed to the same phenomena. Here again, an

increase in masses 2 and 16 was noted by means of the residual gas analyzer. The sample exhibited the same amber discoloration that was obtained by the proton irradiation. The arcing and glow discharge characteristics of the electron irradiation, even though they probably were present, could not be observed because of the brightness of the electromagnetic radiation.

In Fig. 10 the spectral reflectance of the sample is shown as a function of wavelength for various irradiation times. The degradation achieved here is significant and surprising since it is much less than would have been predicted on the basis of the results from the previous individual irradiation experiments. Also of interest is the fact that the combined environment degradation was less than that obtained from the electron irradiation throughout the spectrum with the exception of the short wavelength region around  $0.5 \mu$ .

#### 4.1.6 Combined Environment Effects Summary

One of the principal objectives of this work was to determine if significant combined environment effects (Section I) were observed under these conditions on thermal control coating. Other investigators (Refs. 2, 3, and 5) have reported combined environment effects under the following conditions: (1) vacuum and electromagnetic radiation; (2) vacuum, electron, and electromagnetic radiation, and (3) vacuum, proton, and electromagnetic radiation. However, the validity of past data must be questioned since recent investigators (Refs. 7 and 8) have shown that in situ measurement must be used to obtain accurate data, and in general, past investigators have not used these techniques. The present work differs from the work of past investigators in two respects. The first of these is the fact that the effect of exposure to a test environment was measured exclusively by an in situ technique, and secondly, a different combined environment was used.

In order to summarize the current work Table I (Appendix II) has been prepared to show the percentage of change in reflectance for each test environment at wavelengths of 0.5, 1.0, 1.5, 2.0, and  $2.4 \mu$ . The differences between the sum of the individual effects and the combined environment effects are presented to determine if synergisms are present. There are substantial differences between these two quantities that vary from 7 to 22 percent. Although the combined environment interactions represented here cannot be classified as synergistic, these results are useful for predicting the change in material characteristics achieved in space flights from results in ground facilities. Since it is possible to obtain combined environment effects that are greater than or less than the sum of the individual effects, it seems to be appropriate to

suggest that the synergistic terminology be replaced. These effects could be referred to as combined environment interactions. A specific interaction would then be designated as positive or negative depending on whether the combined environment effect was larger or smaller than the sum of the individual effects.

In order to give an overall picture of the results of the present experiment, the integrated solar reflectance and absorptance were calculated. The solar reflectance was obtained by integrating the spectral reflectance over the solar emission curve. These integrations were performed over the region (from 0.35 to  $2.4 \mu$ ) for which measured spectral reflectance data were available. In an opaque material (transmission equal to zero) such as the present coating, the absorptance (percent) is equal to 100 percent minus the solar reflectance (percent). These data are presented in Table II.

The results of the integrated solar reflectance analysis are in general agreement with those obtained from spectral reflectance values. The combined environment results are less than the sum of the individual exposure effects; in other words, no synergistic results are observed, but a combined environment interaction of a negative 16 percent is obtained.

The integrated solar absorptance data are also in agreement with the previous data in that no synergistic results are present. These data indicate a significant, and larger, combined environment interaction of a negative 36 percent. It would be informative to evaluate the effect of an absorptance error of this magnitude on the spacecraft temperature. In order to determine the significance of this interaction, this error in absorptance can be converted into an equivalent difference in the equilibrium temperature of a spacecraft. Simple heat balance considerations indicate that the temperature of a spacecraft is proportional to the ratio of the solar absorptance of the vehicle surface to the emittance of the surface raised to the one-fourth power. By taking the logarithm and then the differential of such a relation the following equation is obtained by assuming the emittance to remain unchanged.

$$dT = 1/4 \frac{T}{\alpha_s} d\alpha_s$$

where  $T$  is the spacecraft temperature and  $\alpha_s$  is the initial solar absorptance of the surface material. The initial integrated solar absorptance for the combined environment test material was 0.31, and the value at the end of the irradiation period was 0.57. Using these values in the above expression and an initial spacecraft temperature of 300°K, a rise in the spacecraft temperature of 62.9°K is calculated.

On the basis of the data in Table II this is 36 percent lower than would have been calculated from the sum of the effects of the individual exposures. This would correspond to a temperature difference of 22.6°K. Such differences are of engineering significance.

In summary, it can be stated that the combined environment interactions observed in this experiment have produced significant changes in the experimental spectral reflectance of this thermal control material; however, no synergisms have been observed.

## 4.2 RATE EFFECTS

A primary concern with regard to rate effects is the possibility that ground test irradiation rates that are much greater than those in space will produce data that will not be consistent with in-flight results. It is quite possible that there may have to be a trade-off between accelerated ground testing and the production of realistic test results. Very little information is available on this subject, and it is quite important in defining the requirement for ground tests. Rate effects must be evaluated prior to combined environment tests since this could be a cause for some of the interactions that have been associated with test results in this area. Experimental data (Ref. 6) are available that substantiate the fact that accelerated irradiation rates with electromagnetic radiation do produce ground test data that do not agree with in-flight data. One solar constant data, accumulated with in situ techniques, is in excellent agreement with the data of the OSO-00 and OSO-II flights. However, the difference between 1 solar constant, or in-flight data, and data accumulated at intensities of 5, 10, and 20 solar constants increases with increasing intensity.

Only two references have been found for rate effects with protons. One source (Ref. 5) indicates no rate effect for a variation from  $1.1 \times 10^{10}$  to  $1.1 \times 10^{12}$  protons/cm<sup>2</sup>/sec at 100-keV energy level on a titanium dioxide-methyl silicone thermal control coating. Another source (Ref. 14) claimed results on the same coating that are nearly independent of rate. These data were obtained at energies of 50 and 400 keV for a rate variation from  $2 \times 10^{11}$  to  $2 \times 10^{12}$  protons/cm<sup>2</sup>/sec. Consequently, proton irradiation rates in the present tests were maintained at this same level since indications were that there would be no rate effects.

No information has been found that relates to rate effects with electron exposure. In an attempt to obtain preliminary information in this area, sample irradiation with electrons in these experiments was

made at  $6.3 \times 10^{10}$  and  $6.3 \times 10^{11}$  electrons/cm<sup>2</sup>/sec. The results of these experiments are shown in Table III as the difference between the percentage of change in integrated solar absorptance as a function of the time integrated flux (total number of electrons/cm<sup>2</sup>). The striking feature of these data is that the difference as a function of time integrated flux is essentially constant. This implies that the degradation is proceeding at a comparable rate in both cases. This immediately raises the question as to how and when the difference occurred.

If a very simple approach is made to the degradation phenomena, it can be assumed that there are a certain number of sites in the material that, if destroyed or changed by radiation, produce a change in the absorptance. The decrease in these sites would be equal to the probability that a site would be destroyed times the number of sites available times the time:

$$ds = -p s dt$$

where  $s$  is the total number of sites available,  $p$  is the probability that a site will be destroyed, and  $t$  is the time. This, of course, leads to the exponential function

$$s = s_0 e^{-pt}$$

where  $s_0$  is the number of sites available at time zero. This suggests then that a semilogarithmic plot of the absorptance might be informative. In order to determine what may be learned from such a plot, all irradiation runs are plotted for comparison in Fig. 11 showing the increase in absorptance with time.

The electromagnetic and the proton irradiation data seem to fit this type of plot reasonably well and extrapolate back to the measured absorptance value at time zero. This is not completely true for the other irradiation runs. These data apparently are exponential in nature, but the extrapolated intercept of these plots is not equal to the absorptance at time zero. The low intensity electron curve intercept is displaced by +0.1 absorptance units, whereas the higher intensity curve intercept is displaced by +0.17. It is possible that this intercept displacement is a measure of the rate effect and that it can be qualitatively related to observed physical phenomena (Section 4.1.3). It has been pointed out previously that arcing and glow discharge phenomena were observed during the electron irradiations. Qualitatively, this activity was apparently more intense at the higher irradiation rate. If the damage production from these phenomena decays exponentially to a negligible value within the first 10 to 15 percent of a run, so that a second mechanism would be the dominant producer of degradation, this

would agree qualitatively with the experimental picture suggested by these plots. If such an intercept displacement is a result of only the electron irradiation, such a displacement should also occur and does on the combined environment plot. Although a high electron irradiation rate was used in the combined test, the displacement of the intercept is more nearly characteristic of that achieved with the lower irradiation rate. This may be qualitatively explained if it is assumed that the short-term damage is a function of charge storage in the material. In the presence of protons this charge storage effect is partially neutralized and this activity proceeds at a reduced rate. If subsequent experimental work substantiates this speculative picture, it would appear that the combined environment interaction can be directly attributed to the electron rate effect and that by a reduction in irradiation rate the difference between the sum of the individual effects and the combined effects may become negligible.

In summary it can be said that experimental effects have been observed that are directly related to the electron irradiation rate.

#### 4.3 BLEACHING

Other investigators (Refs. 4, 5, 7, and 8) have demonstrated that irradiated thermal control coatings may recover when exposed to air. This phenomenon has been referred to as bleaching. It is this consideration that makes it mandatory to utilize in situ measurement techniques. Of importance to testing is the minimum level that must be maintained on constituents such as  $O_2$  in order to prevent bleaching while the experiment is in progress. No known information has been found on this subject that can be related to high vacuum conditions.

In order to determine if there was a bleaching problem under test conditions, the samples irradiated by electromagnetic radiation, electrons, and protons were respectively allowed to soak in the test environment for periods of 3 and 7 days, 8 days, and 5.5 hr. No detectable change in the reflectance of the samples was noted, so the test environment was considered satisfactory.

In order to substantiate the bleaching reported by other investigators, all irradiated samples were exposed to 0.2-torr partial pressure of oxygen followed by a 220-hr exposure to ambient air. The results of these experiments are shown in Figs. 12 to 15. None of the severely degraded samples achieved complete recovery; however, the recovery was substantial in every case. The electromagnetic degradation was very slight, and this sample did essentially achieve full recovery.

These data reaffirm the present need for in situ measurement techniques, and have demonstrated that the test environment is satisfactory for this type of testing.

#### 4.4 STRUCTURE EXAMINATION

Irradiation damage that results in a degradation of the spectral reflectance of the present thermal control rating can occur through damage to methyl silicone binder, the titanium dioxide pigment, or both. Decomposition products from either reaction can possibly enhance the rate of degradation (Ref. 15). Investigators (Refs. 9 and 16) in this field indicate that both modes of damage are possibly present. During the present experiment the capability was not available to examine changes occurring in the titanium dioxide. However, it was felt that changes in the methyl silicone binder might be detected by examining the infrared spectra. The infrared spectra of both the non-irradiated and irradiated material is shown in Figs. 16 to 21 where the transmittance (percent) is plotted as a function of wavelength in microns. Figure 16 is the nonirradiated reference spectra of the methyl silicone showing the characteristic silicone structure associated with specific portions of the spectra. The only indications of structure change are found on the low rate electron run (Fig. 17) and to a lesser extent on the proton run (Fig. 18). Changes in the 3.4- and 8- $\mu$  bands indicate a depletion in the methyl group ( $\text{CH}_3$ ). It is quite surprising that this does not appear in all spectra since the experimental outgassing data indicated a buildup in masses 16 and 2 which could be attributed to structure changes from the irradiation forming methane ( $\text{CH}_4$ ) and hydrogen ( $\text{H}_2$ ).

It should be pointed out that these samples were exposed to the atmosphere prior to the infrared measurement, and it is possible that this procedure has biased these results so that definite indications of structure change are not possible. Possibly these measurements should also be made in situ.

#### 4.5 MICROSCOPIC EXAMINATION

Photomicrographs were taken of the samples at 100 and 200 power magnification. Surface photomicrographs are shown in Fig. 22, and the cross-section photographs are shown in Fig. 23. A lack of definition in the photographs makes it desirable to supplement the photographs by visual observation. The coatings are of the order of 0.004 in. (100  $\mu$ ) thick.

#### 4.5.1 Nonirradiated Sample

The surface of the sample is smooth, as indicated by both photographs (Figs. 22a and 23a). The dark spots on the surface are dust particles that are difficult to dislodge because of the nature of the material. To the eye, the surface appears to be dimpled; an indication of this may be obtained by carefully looking at the surface in the cross section which corresponds to sunken portion of a dimple.

#### 4.5.2 Electromagnetic Radiation Sample

Extremely fine roughening of the surface was the only visible indication of damage (Figs. 22b and 23b). This was determined by visual observation and is supported by the cross-section photograph (Fig. 22b).

#### 4.5.3 Electron Irradiated Sample

The general characteristic of the radiation damage for the low irradiation rate is a general roughening of the surface (Figs. 22c and 23c); this is more severe than that resulting from electromagnetic radiation. The light and dark areas in the cross section (Fig. 23c) have no meaning; they are a result of the preparation technique.

The results of the high irradiation rate run are very pronounced (Figs. 22d and 23d). The general surface roughening is more severe, and there are signs of significant erosion. In the surface photograph (Fig. 22d), near the bottom, the white streaks and dark areas represent heavily eroded areas. The dark areas represent an absence of a coating, and the white areas are small mounds of the coating. The photograph of the cross section (Fig. 23d) gives an excellent picture of this erosion.

#### 4.5.4 Proton Irradiation Sample

Probably the most spectacular of all these samples was the proton irradiated coating. There was general surface roughening but this was overshadowed by the large amount of surface cracking. The surface photograph (Fig. 22e) gives the appearance that some of these cracks are wide and deep. This is not the case; these wide dark areas are sloping depressions that terminate in a small crack. The surface is white all through these dark areas. In the cross section photograph (Fig. 23e) the coating appears dark because of the lighting and exposure time. The fine dark lines running from the top to the bottom of the coating are cracks that originate in the dark areas on the surface photograph. The cracks may have been produced by thermal stress at the

coating surface since the ionization capability of the protons is much less than that of the electrons, causing a large percentage of the total energy to be dissipated in the form of thermal energy. This energy will be concentrated in less than 1 percent of the total volume of the coating since the proton penetration depth is of the order of  $0.35 \mu$  ( $\sim 100 \mu$  thick).

#### 4.5.5 Combined Environment Sample

The sample exposed to the combined environment shows a combination of the three types of damage observed in the other samples (Figs. 22f and 23f). This consists of cracking, surface roughening, and erosion. The most striking feature of this photograph is the reduction in the surface cracking as compared to the proton irradiation.

### SECTION V CONCLUDING REMARKS

A combined environment research chamber has been described and evaluated on the basis of the performance during a limited combined environment test. The irradiation capability, multisample holder, in situ measurement technique, and the noncontaminating and nonbleaching test environment have been shown to be adequate for this type of research. It was hoped that, in addition to the chamber evaluation, some experimental contribution could be made to the state of the art in combined environment testing. The investigation of the existence of significant synergistic effects and irradiation rate effect with in situ measuring techniques was the principal objective of the experimental work. These results are summarized by the following statements:

1. No effects were observed that could be classed as synergistic. However, a combined environment interaction was observed wherein the combined environment effect was less than the sum of the effects from the constituents of this environment.
2. An irradiation rate effect was measured for the electrons. Greater optical degradation was achieved at the higher electron rate for the same integrated flux.
3. No bleaching or contamination of test samples was detected under test conditions.
4. Physical phenomena associated with the irradiation of the thermal control coating are general surface roughening and cracking, discoloration, and outgassing.

One speculative comment that may be made on the basis of the limited work presented in this report is that the observed combined environment interaction is directly attributable to the electron rate effect. It is also quite possible that a reduction in irradiation rate, which would not preclude accelerated testing at a lower rate, would eliminate the combined environment interaction effect. On the basis of these speculative comments and the measured rate effect, it is recommended that future combined environment testing be preceded by a rate effects investigation in order to ensure that realistic rates will be used in investigating this problem.

## REFERENCES

1. Kirby, W. G. and Kindall, S. M. "Problems in the Laboratory Simulation of Space Particulate Radiation." AEDC-TR-66-131 (AD804214), December 1966.
2. Hammel, R. L. "Low Energy Radiation Damage to Surfaces." TRW Space Technology Laboratories.
3. Breuch, R. A. "Exploratory Trapped-Particle and Trapped-Particle-Plus-Ultraviolet Effects on the Optical Properties of Spacecraft Thermal Control Coatings." AIAA Paper No. 65-646. Thermophysics Specialist Conference, September 1965.
4. Babjak, S. J., Boebel, C. P., and Tweedie, A. T. "Combined Space Environmental Effects on Thermal Control Coatings." IEEE Annual Conference on Nuclear and Space Radiation Effects, July 1966.
5. Pinson, J. D. "Synergistic and Accelerated Testing Effects On Space Thermal Control Coating." Thesis, Doctor of Philosophy, Oklahoma State University, Stillwater, Oklahoma, May 1966.
6. Greenberg, S. A. Lockheed Missiles and Space Company, private communication, 1967.
7. Farnsworth, D. "Simultaneous Vacuum-Ultraviolet Exposure with Radiative Property Measurements." Twelfth National Vacuum Symposium, September 1967.
8. Douglas, H. J., Breuch, R. A., McCargo, M., and Starkey, R. D. "Solar Wind-Plus-Ultraviolet Exposure Studies on Spacecraft Thermal Control Coatings Using In Situ Optical Property Measurement Techniques." AIAA Space Simulation Conference, September 1967.

9. Jacquez, J. A. and Kuppenheim, H. F. "Theory of the Integrating Sphere." Journal of the Optical Society of America, Vol. 45, No. 6, June 1955, pp. 460-470.
10. Southerlan, R. E., Frazine, D. F., and Cox, G. S. "Combined Space Environmental Effects on Spacecraft Coating." AEDC-TR-68-114, June 1968.
11. "Application Data and Accessory Equipment for Use With A-H6 and B-H6 Mercury Lamps." GET-1248-C, General Electric Company, Lynn, Massachusetts.
12. Mole-Richardson Co. "Pyrometric Molarc Lamp Type 2371." Bulletin No. 2371, Hollywood, California.
13. Space Materials Handbook, ML-TDR-64-40, AF Materials Laboratory, Air Force Systems Command, January 1965.
14. Miller, R. A. and Campbell, F. J. "Effects of Low Energy Protons on Thermal Control Coatings." AIAA Paper No. 65-648, AIAA Thermophysics Specialist Conference, Monterey, California, September 1965.
15. Rausa, G. "Ultraviolet Radiation Induced Effects in Some Optical Materials." AIAA Thermophysics Specialist Conference, April 1967.
16. Jorgenson, G. V. "Effects of Simulated Solar-Wind Bombardment on Spacecraft Thermal Control Surfaces." AIAA Thermophysics Specialist Conference, September 1965.

**APPENDIXES**  
**I. ILLUSTRATIONS**  
**II. TABLES**

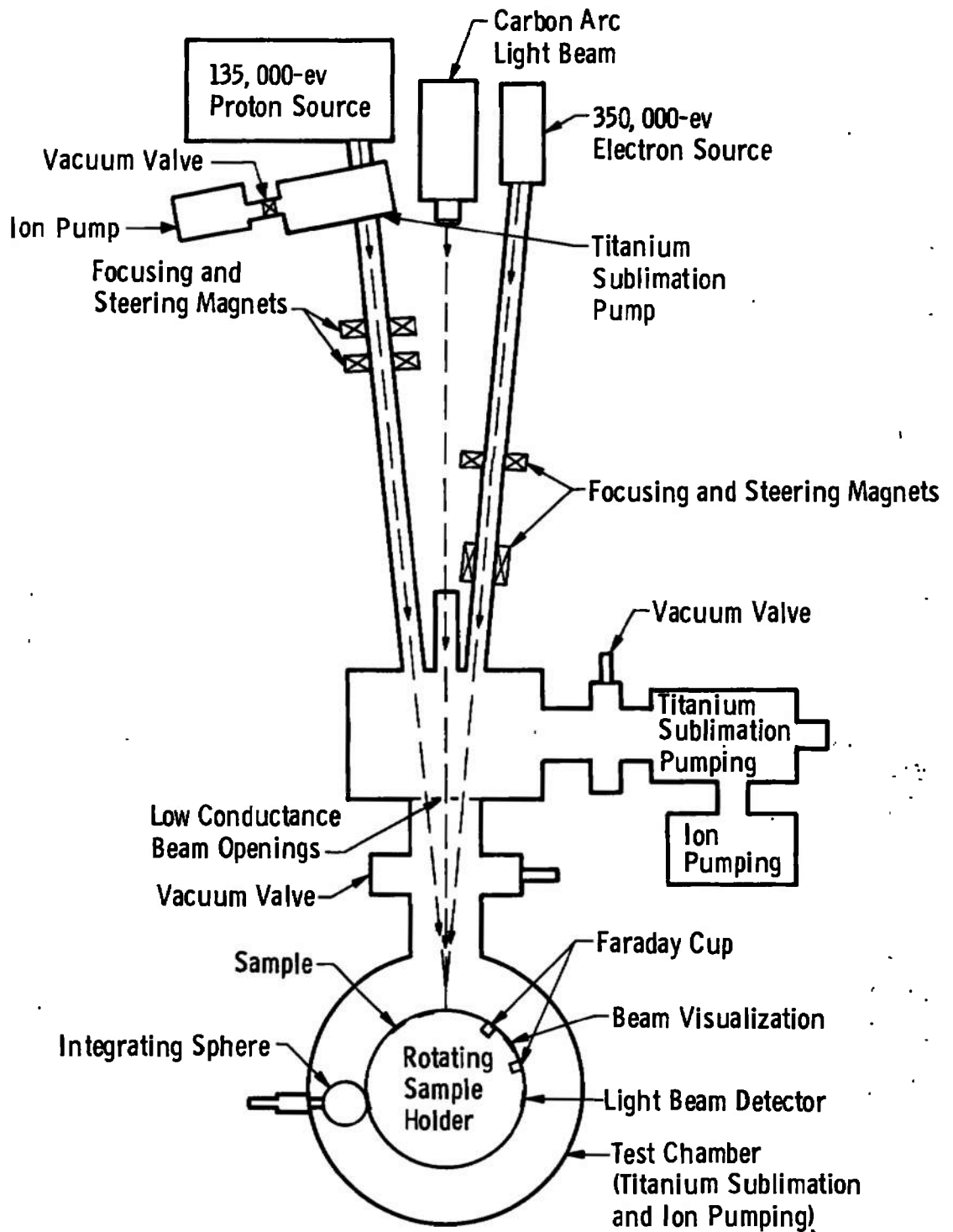
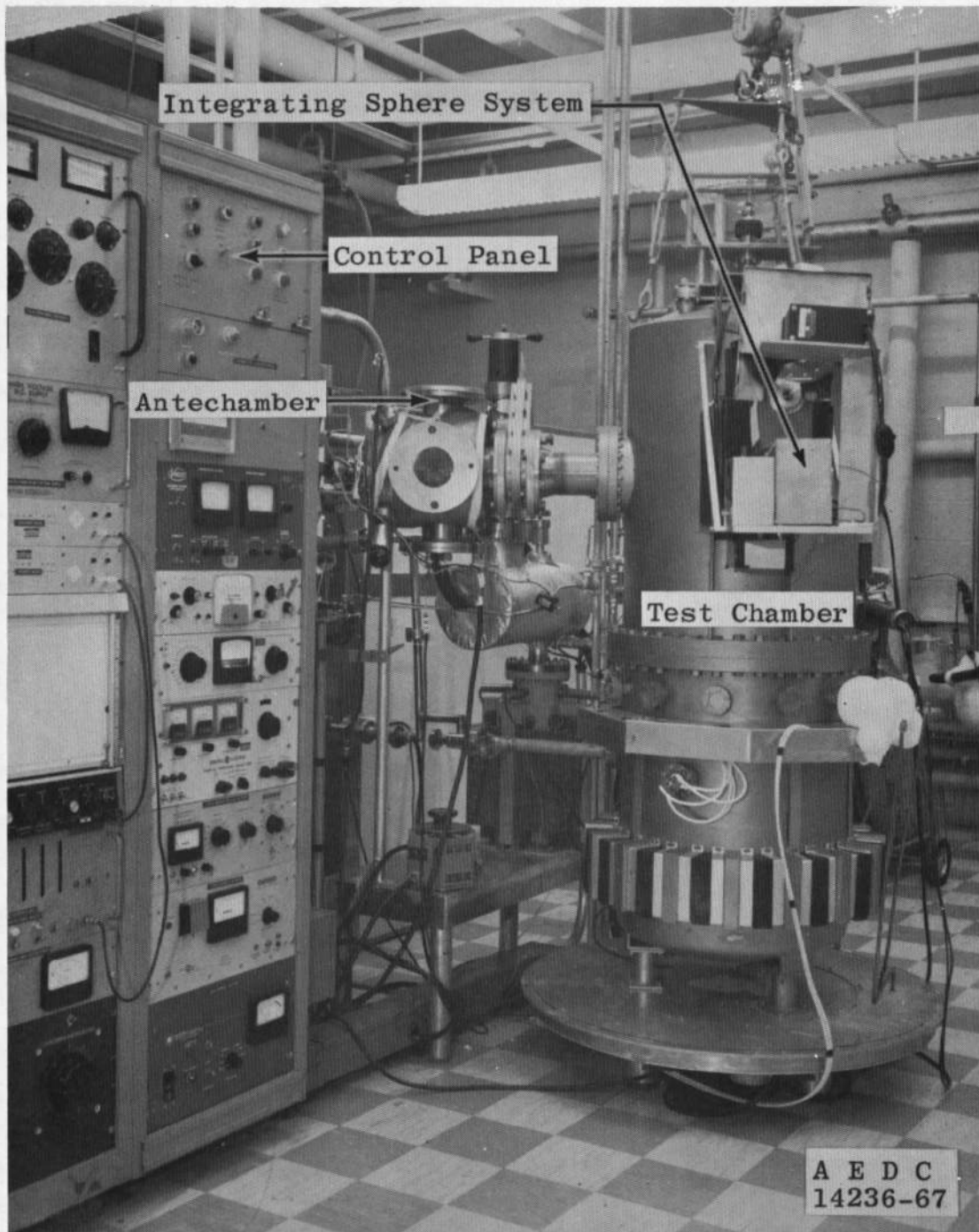


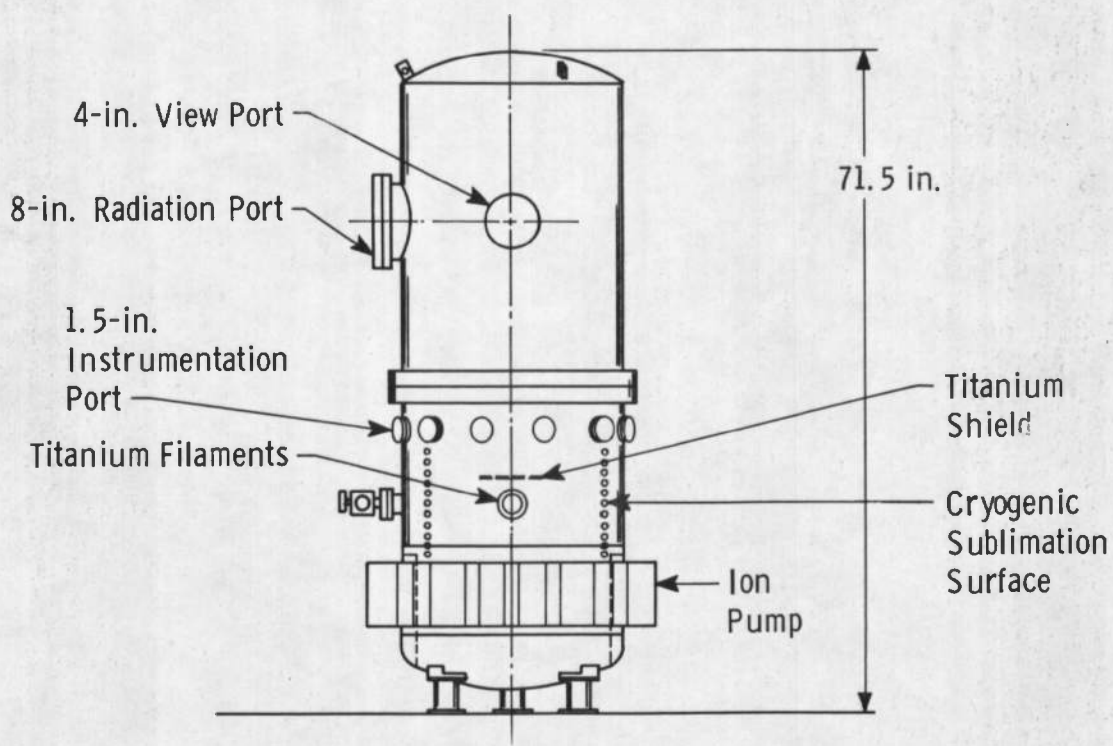
Fig. 1 Schematic of the Combined Environment Test Chamber



a. Photograph

Fig. 2 Combined Environment Chamber

Component	Volume, litres	Surface Area, in. <sup>2</sup>
Pump	237	2927
Bell Jar	267	3172
Total	524	6099
<u>Performance</u> $5 \times 10^{-11}$ torr in 24 hr with Bakeout		



b. Elevation Drawing  
 Fig. 2 Concluded

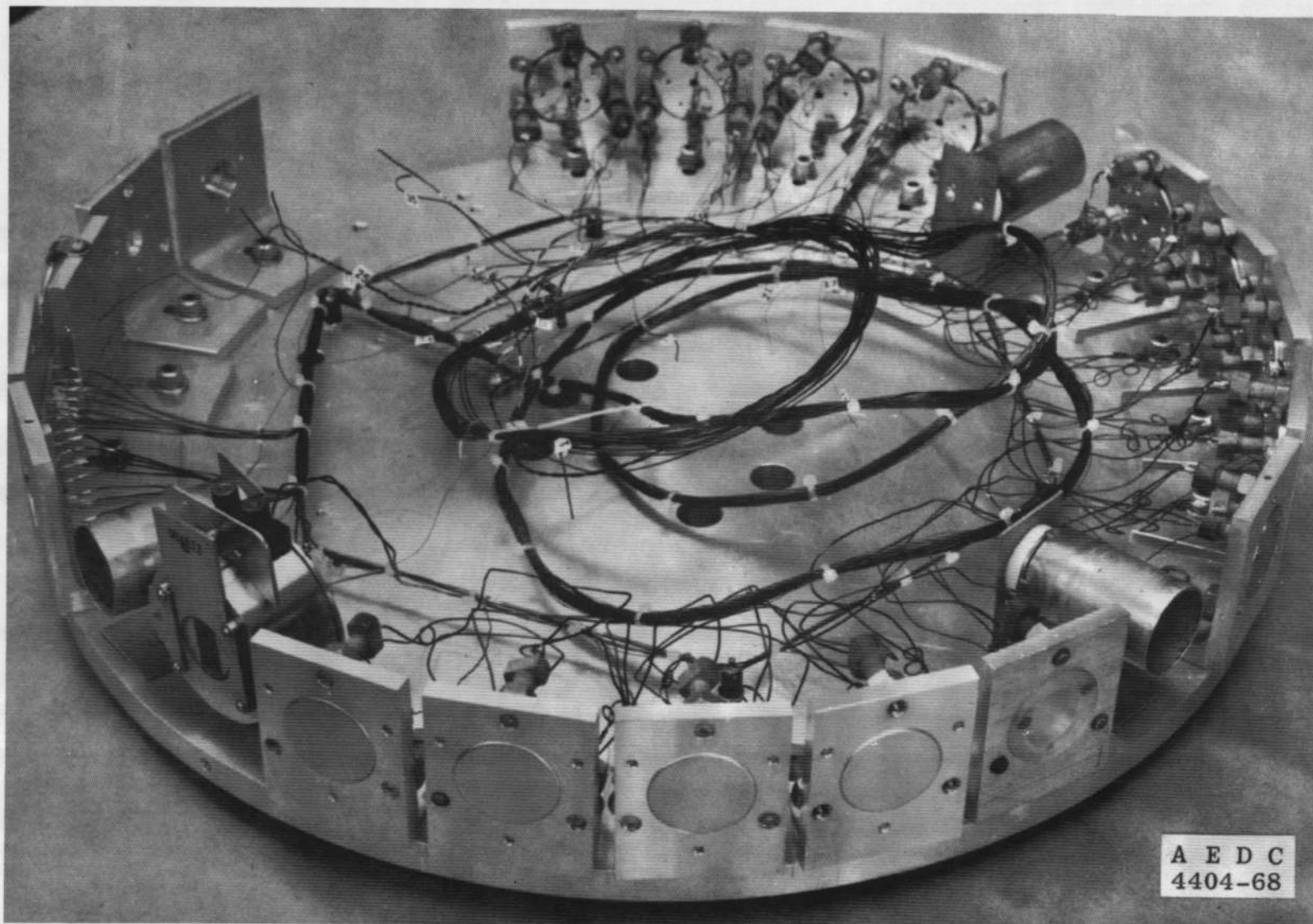


Fig. 3 Combined Environment Sample Holder

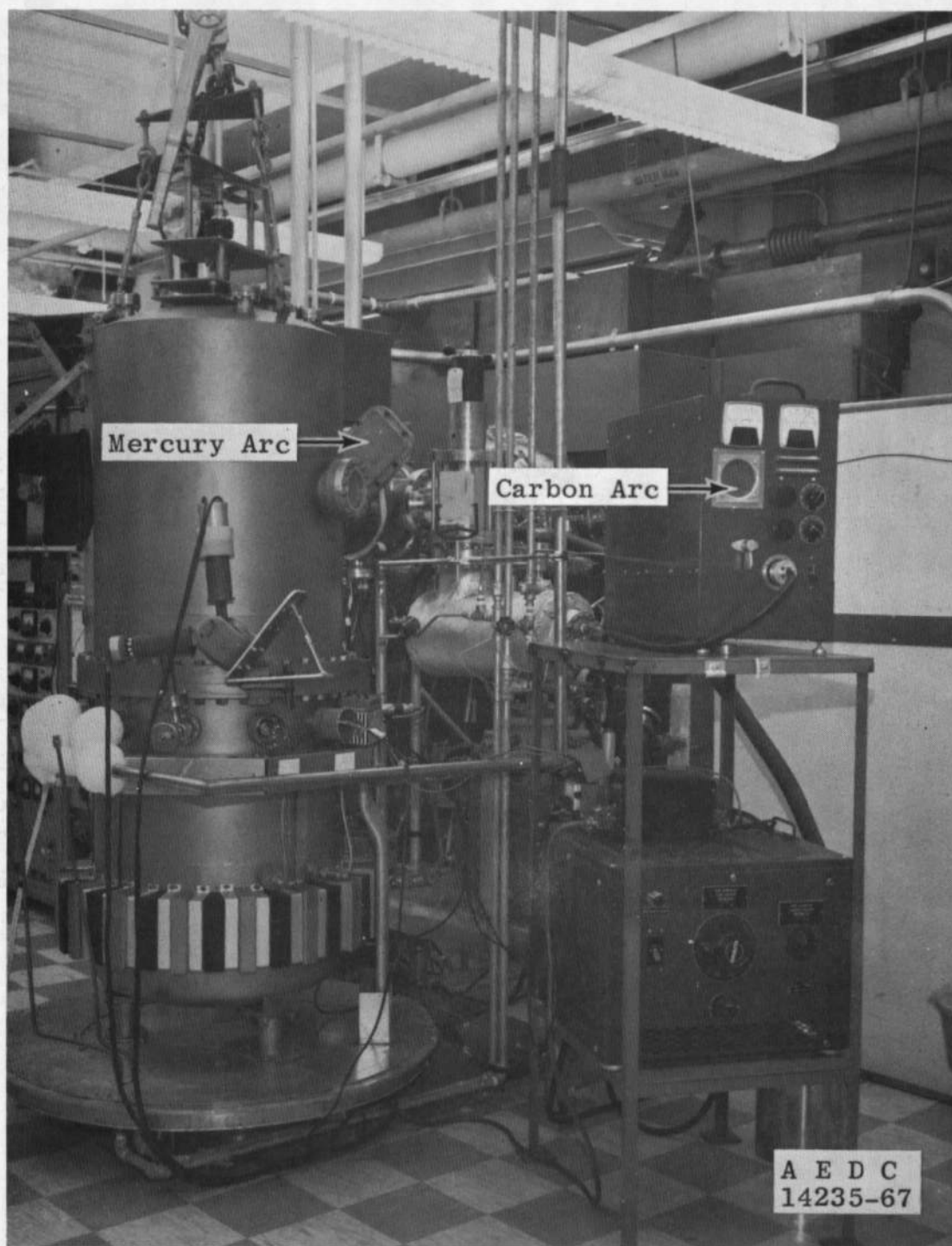


Fig. 4 Carbon and Mercury Arc Lamps

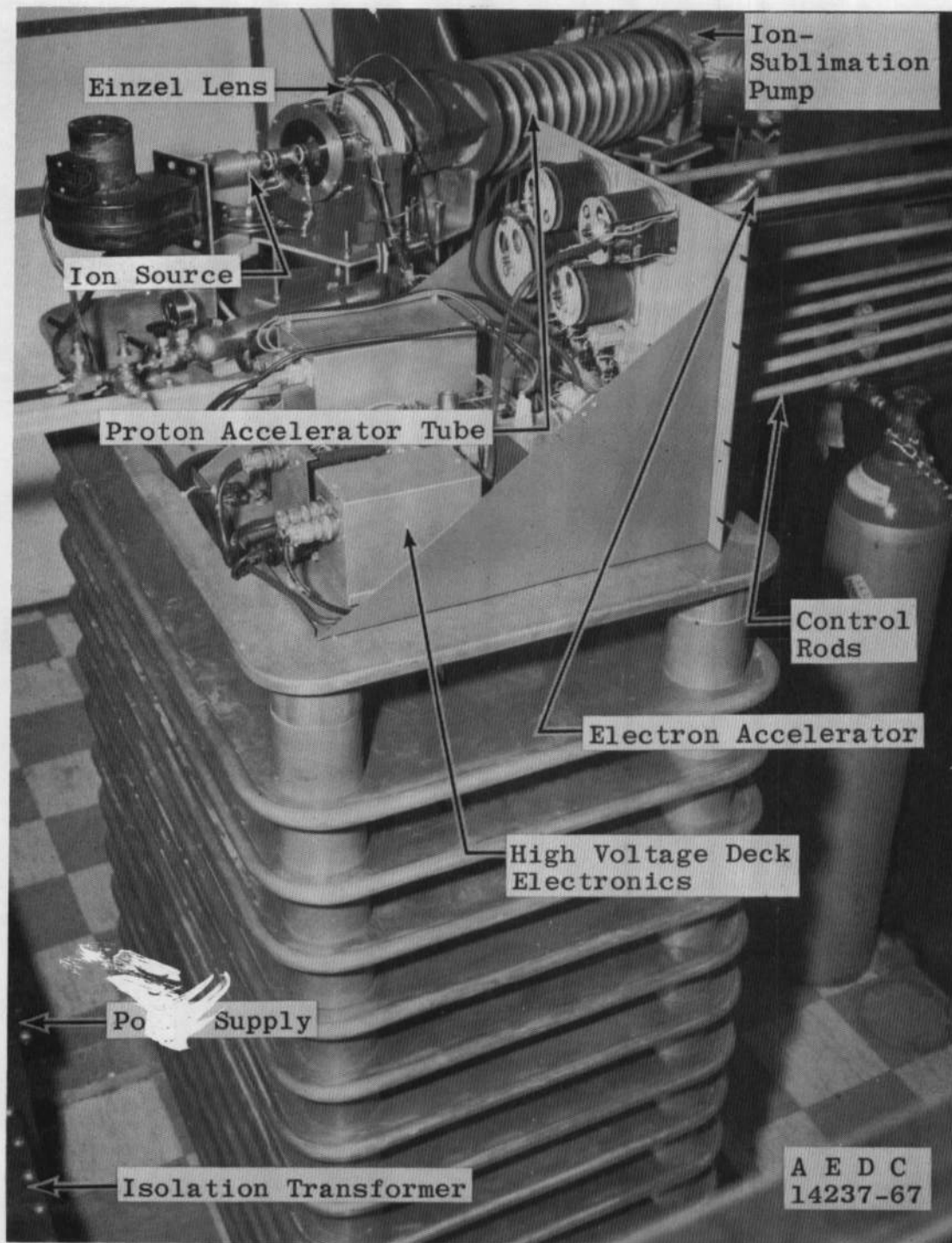


Fig. 5 Proton and Electron Accelerator

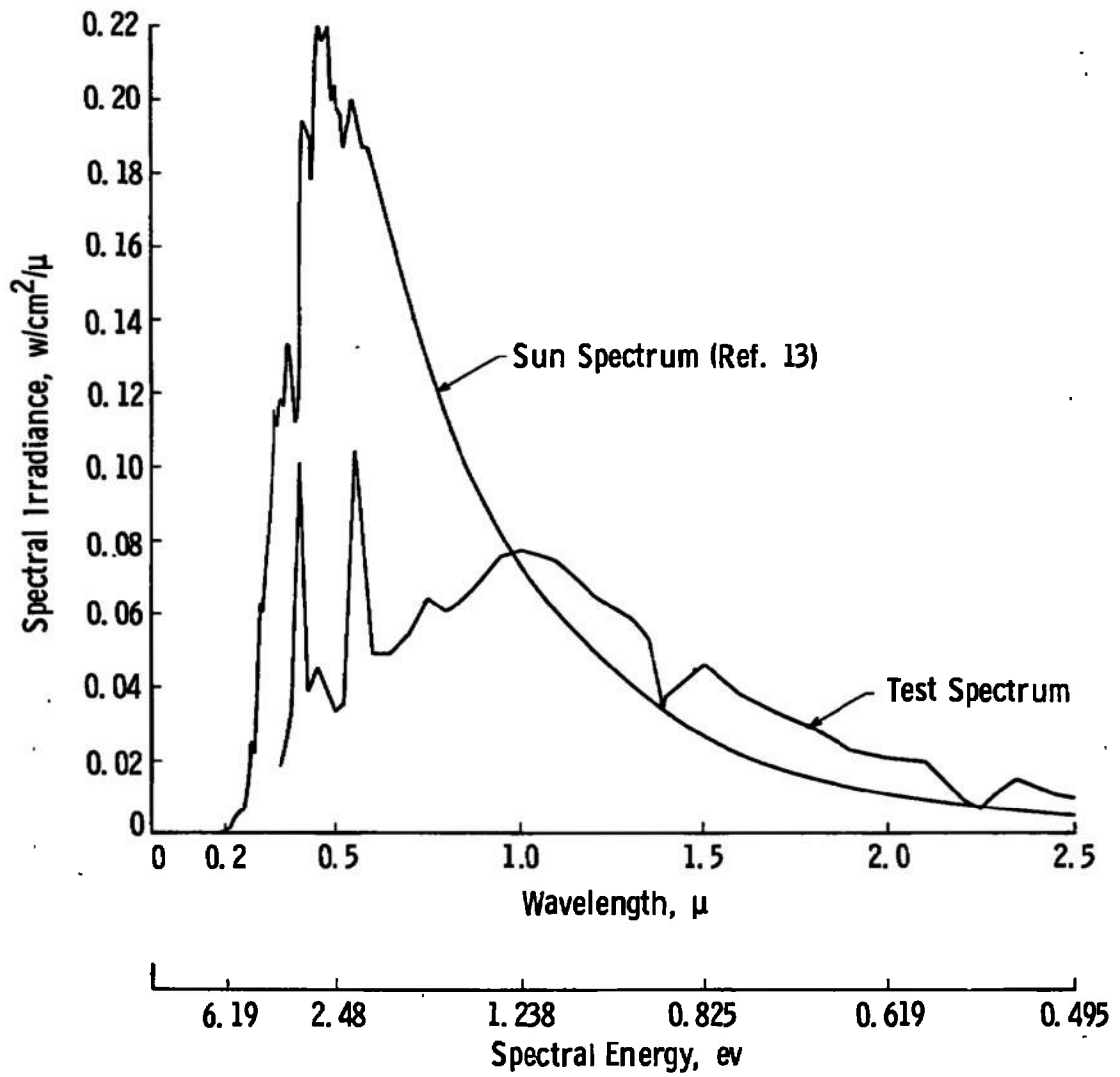


Fig. 6 Spectral Irradiance of the Electromagnetic Test System and the Sun

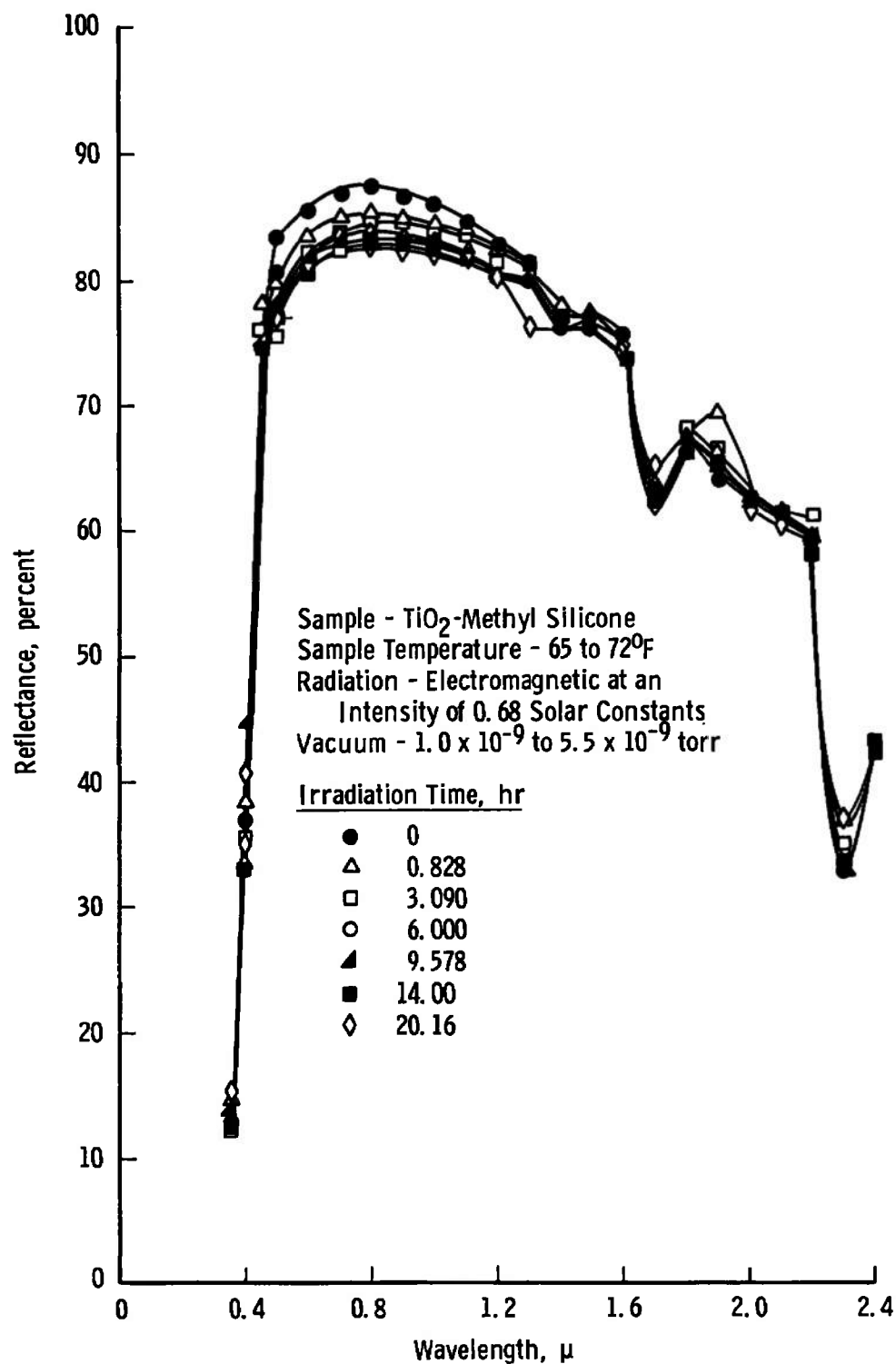


Fig. 7 Optical Degradation of  $\text{TiO}_2$ -Methyl Silicone Thermal Control Coating from Electromagnetic Radiation

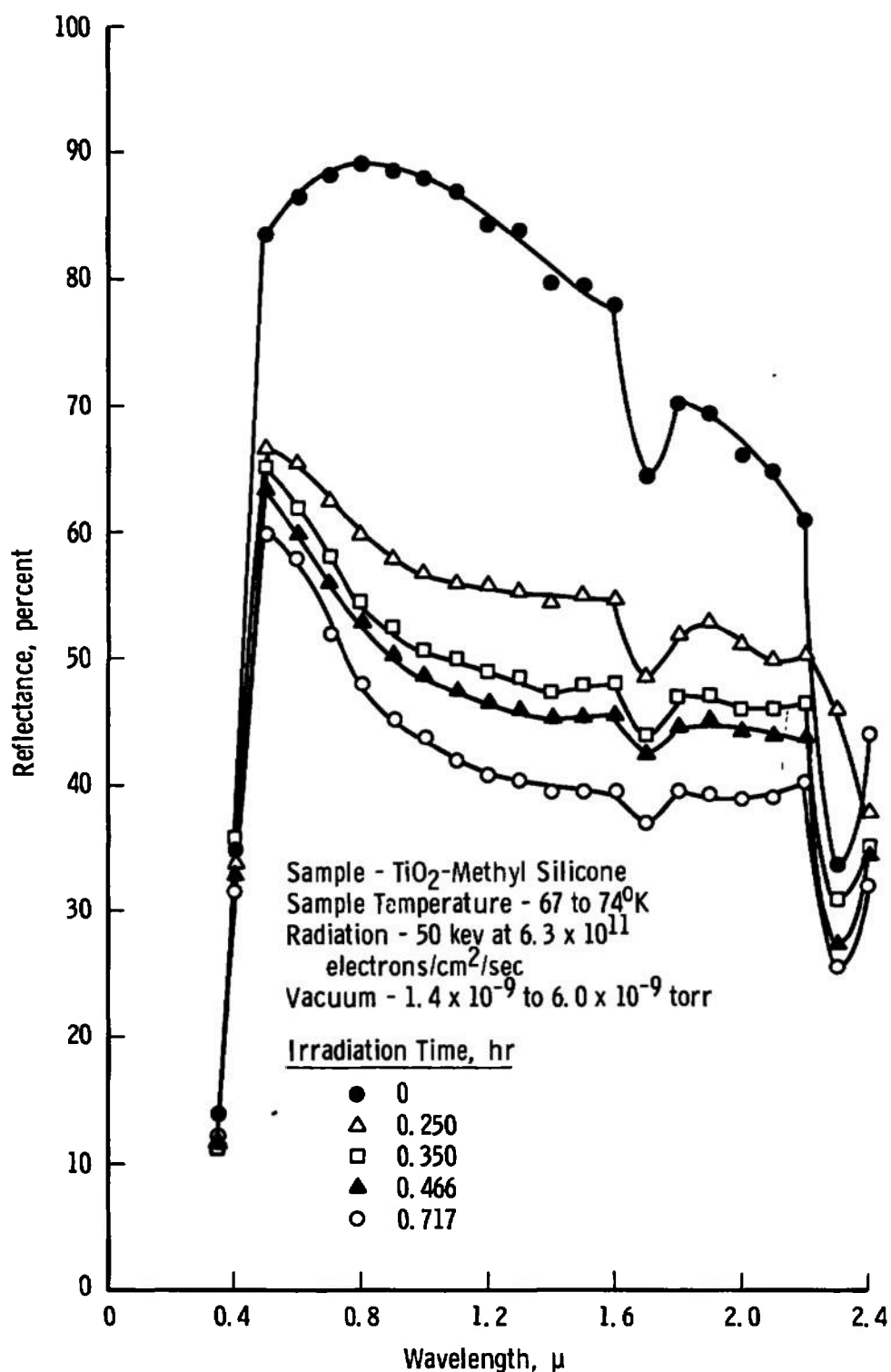


Fig. 8 Optical Degradation of  $\text{TiO}_2$ -Methyl Silicone Thermal Control Coating from Electron Irradiation

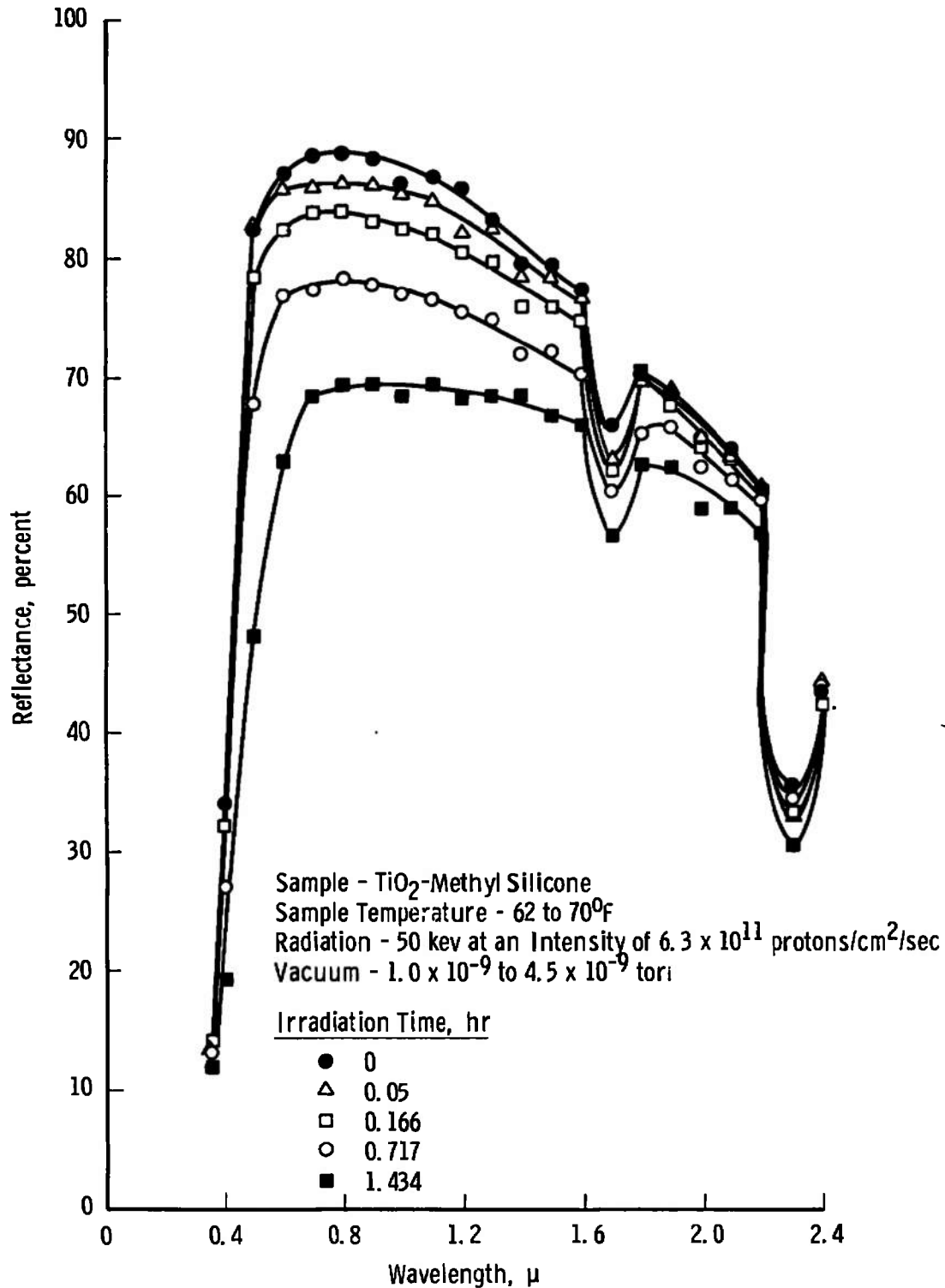


Fig. 9 Optical Degradation of  $\text{TiO}_2$ -Methyl Silicone Thermal Control Coating from Proton Irradiation

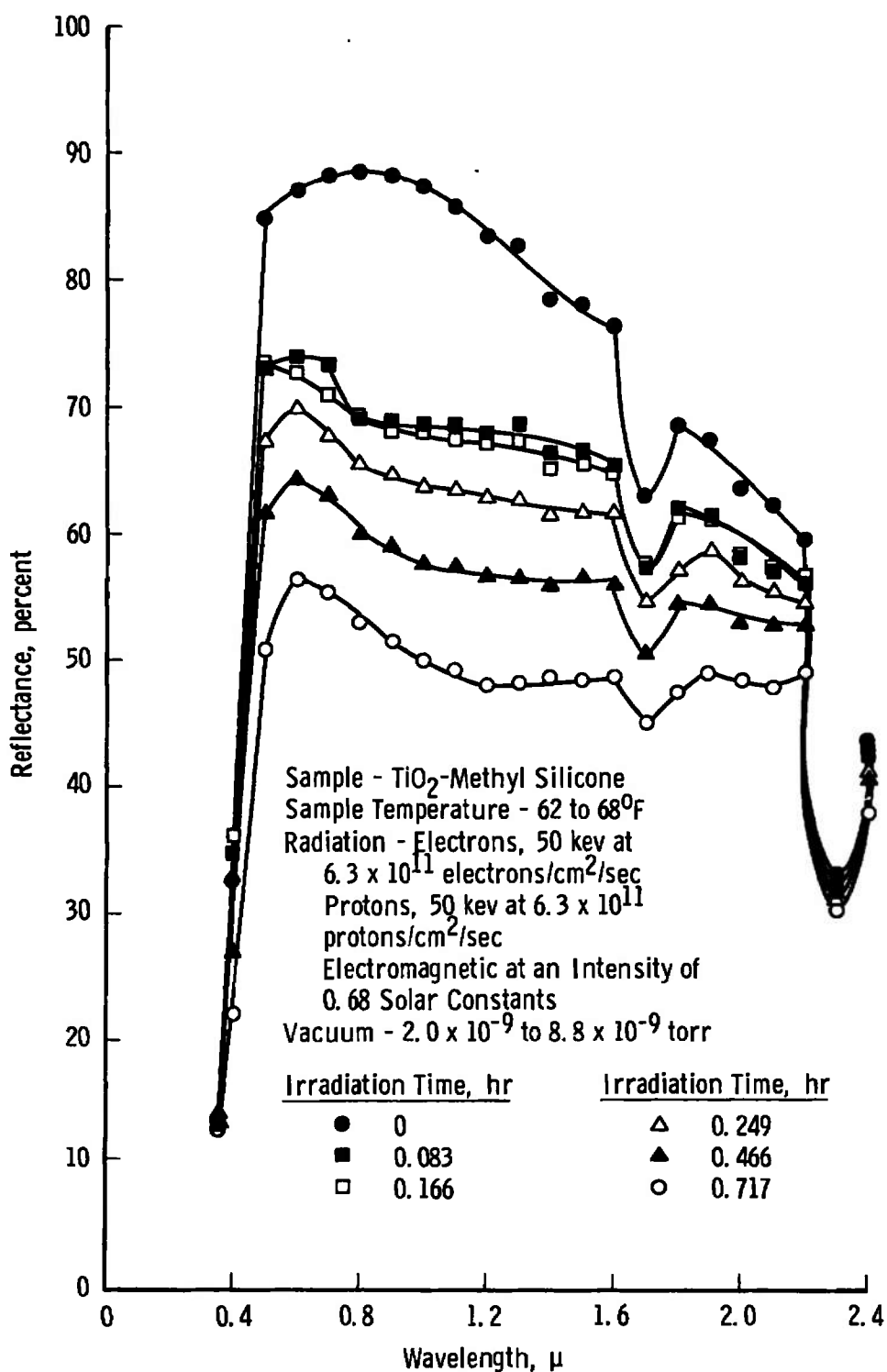


Fig. 10 Optical Degradation of  $\text{TiO}_2$ -Methyl Silicone Thermal Control Coating from Simultaneous Electron, Proton, and Electromagnetic Irradiation

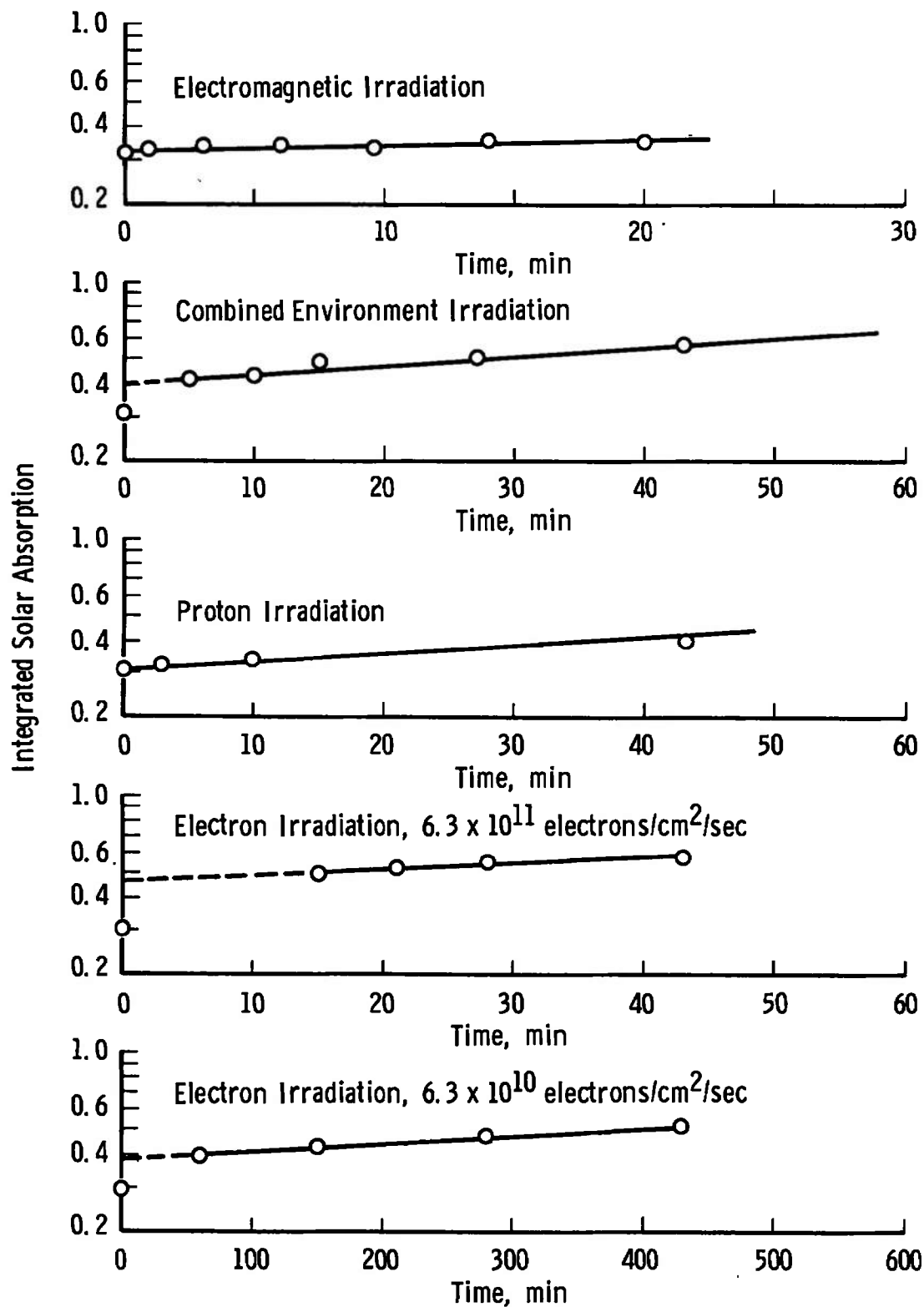


Fig. 11 Integrated Solar Absorption versus Irradiation

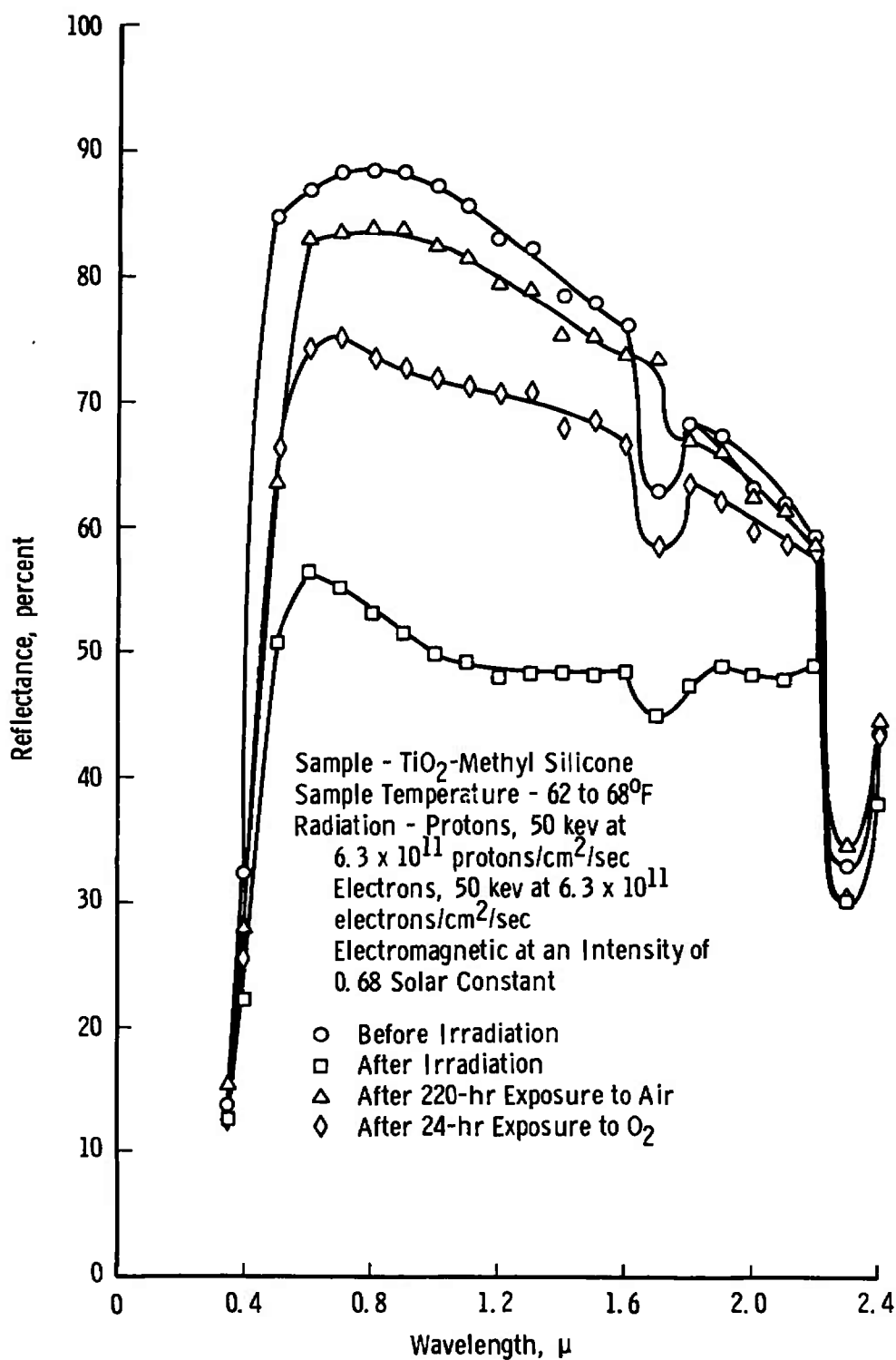


Fig. 12 Recovery of Combined Environment Irradiated  $\text{TiO}_2$ -Methyl Silicone Thermal Control Coating upon Exposure to  $\text{O}_2$

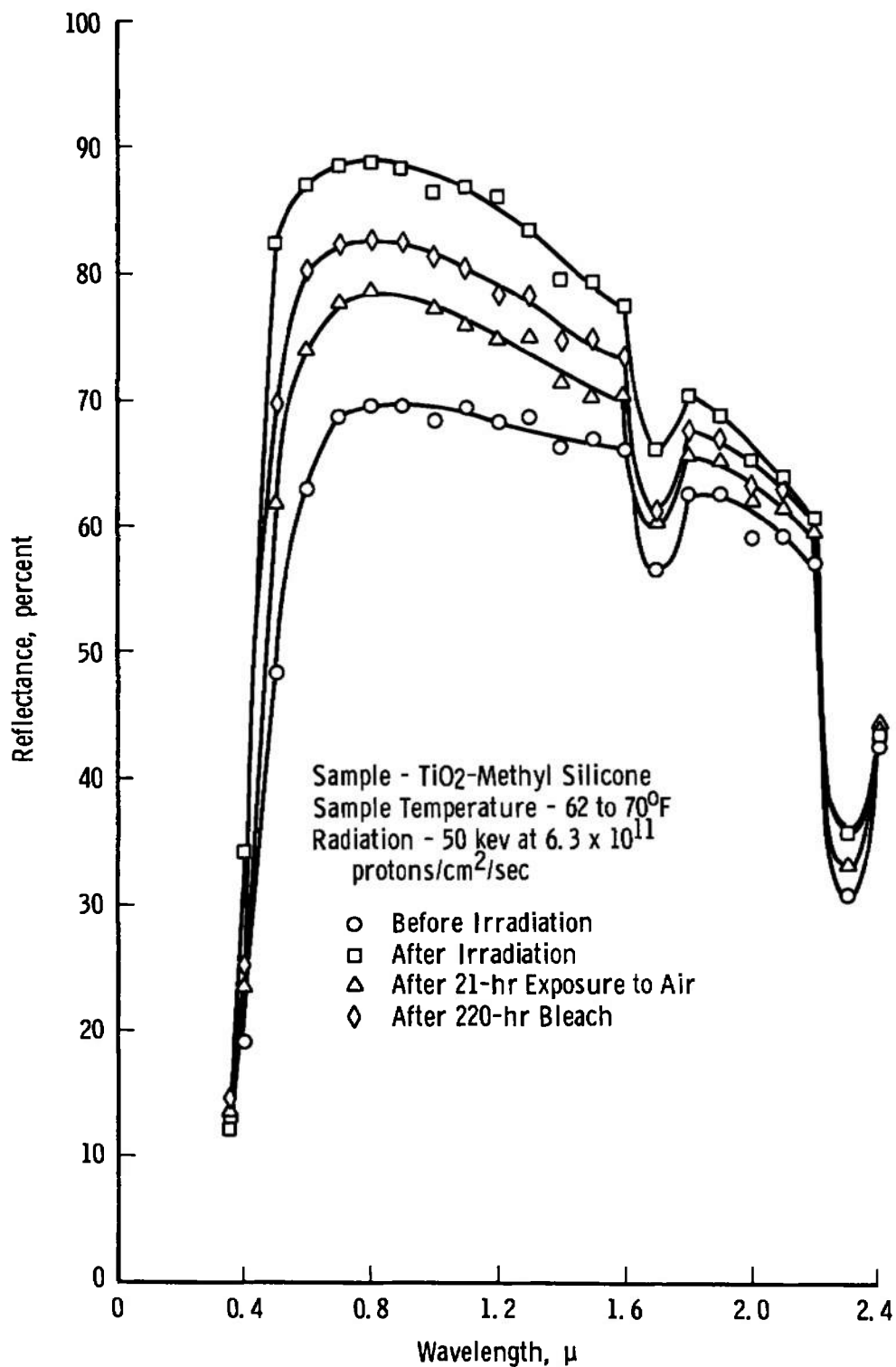


Fig. 13 Recovery of Proton Irradiated  $\text{TiO}_2$ -Methyl Silicone Thermal Control Coating upon Exposure to  $\text{O}_2$

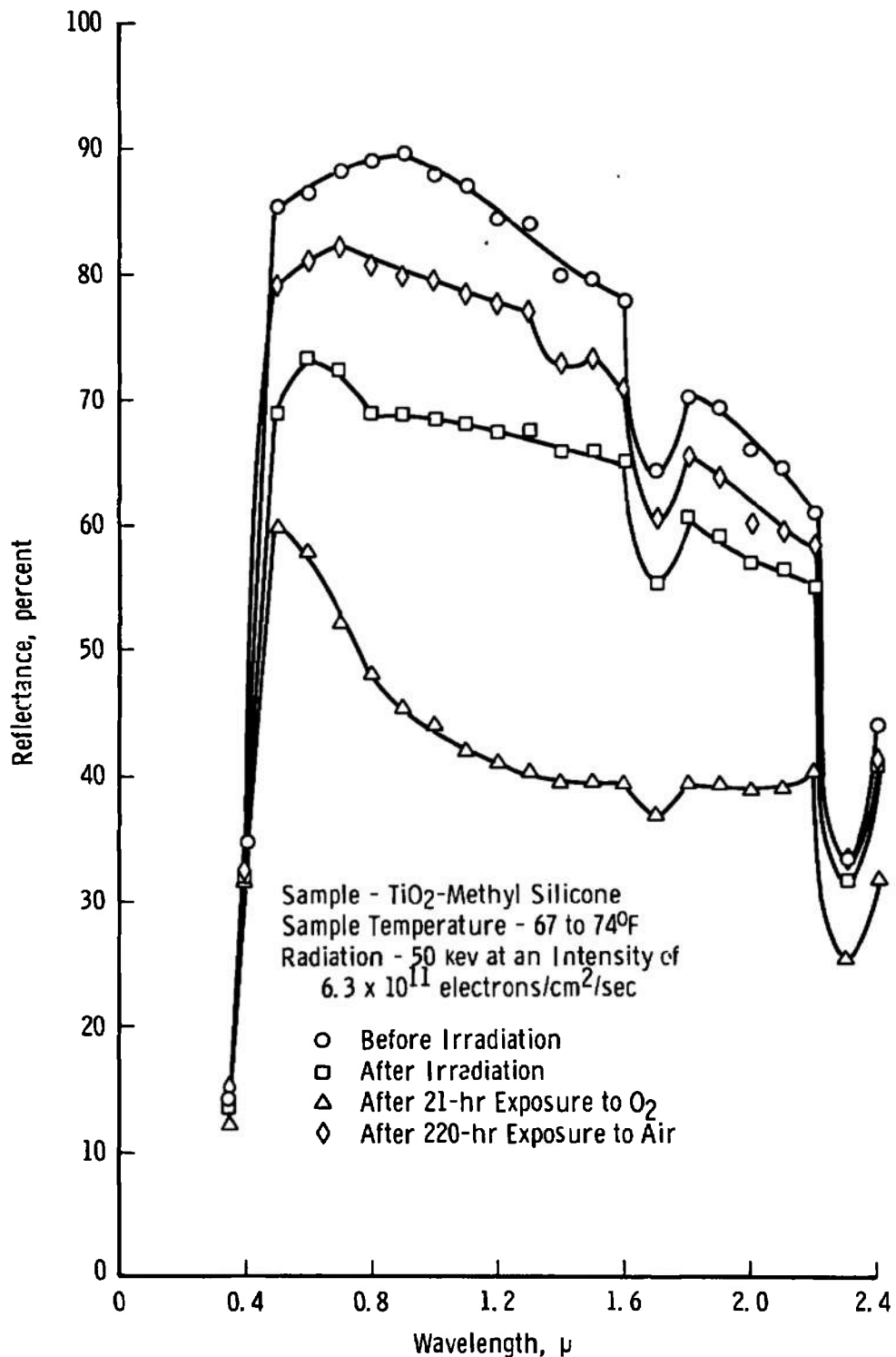


Fig. 14 Recovery of Electron Irradiated  $\text{TiO}_2$ -Methyl Silicone Thermal Control Coating upon Exposure to  $\text{O}_2$

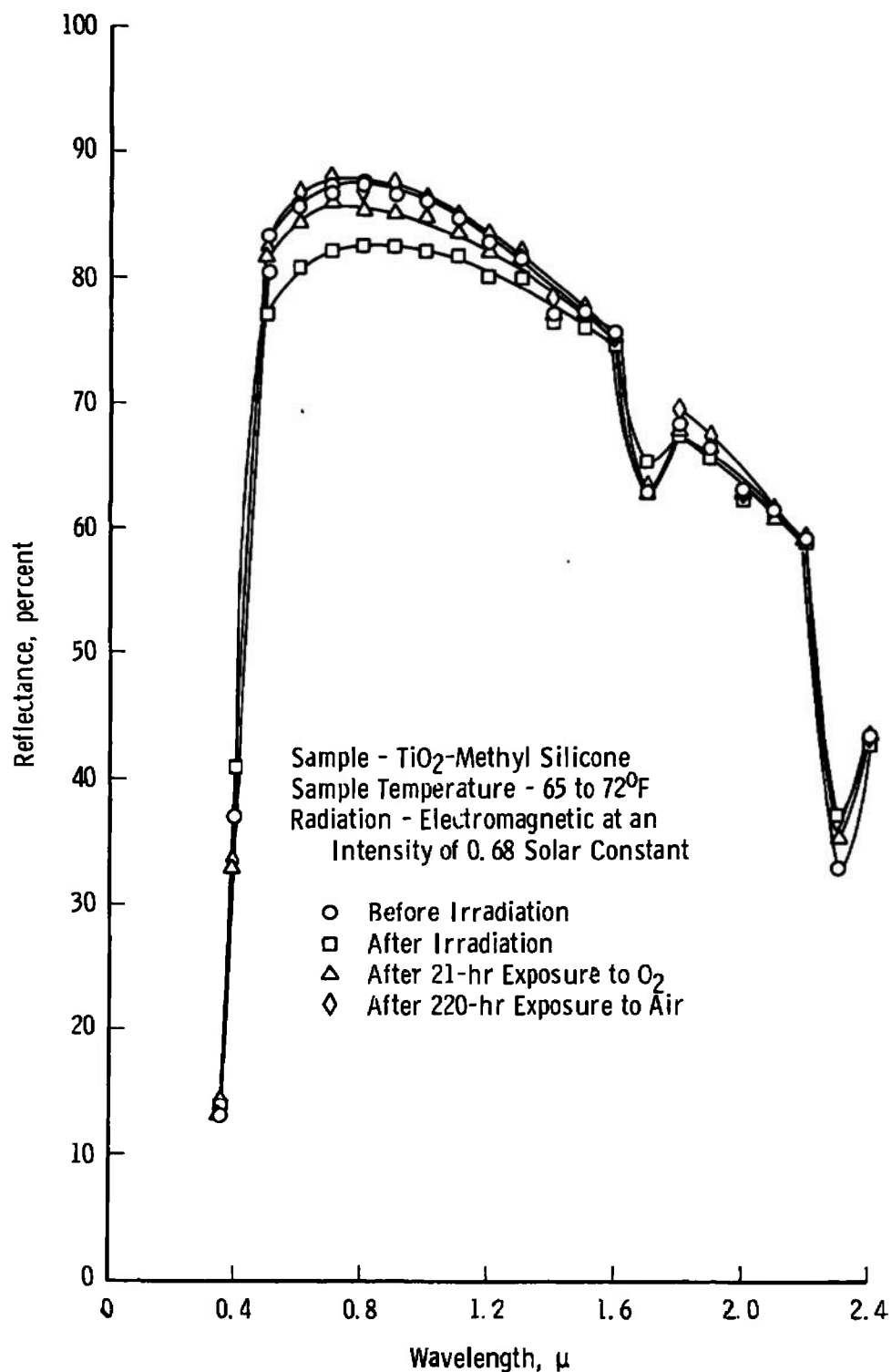


Fig. 15 Recovery of Electromagnetic Irradiated  $\text{TiO}_2$ -Methyl Silicone Thermal Control Coating upon Exposure to  $\text{O}_2$

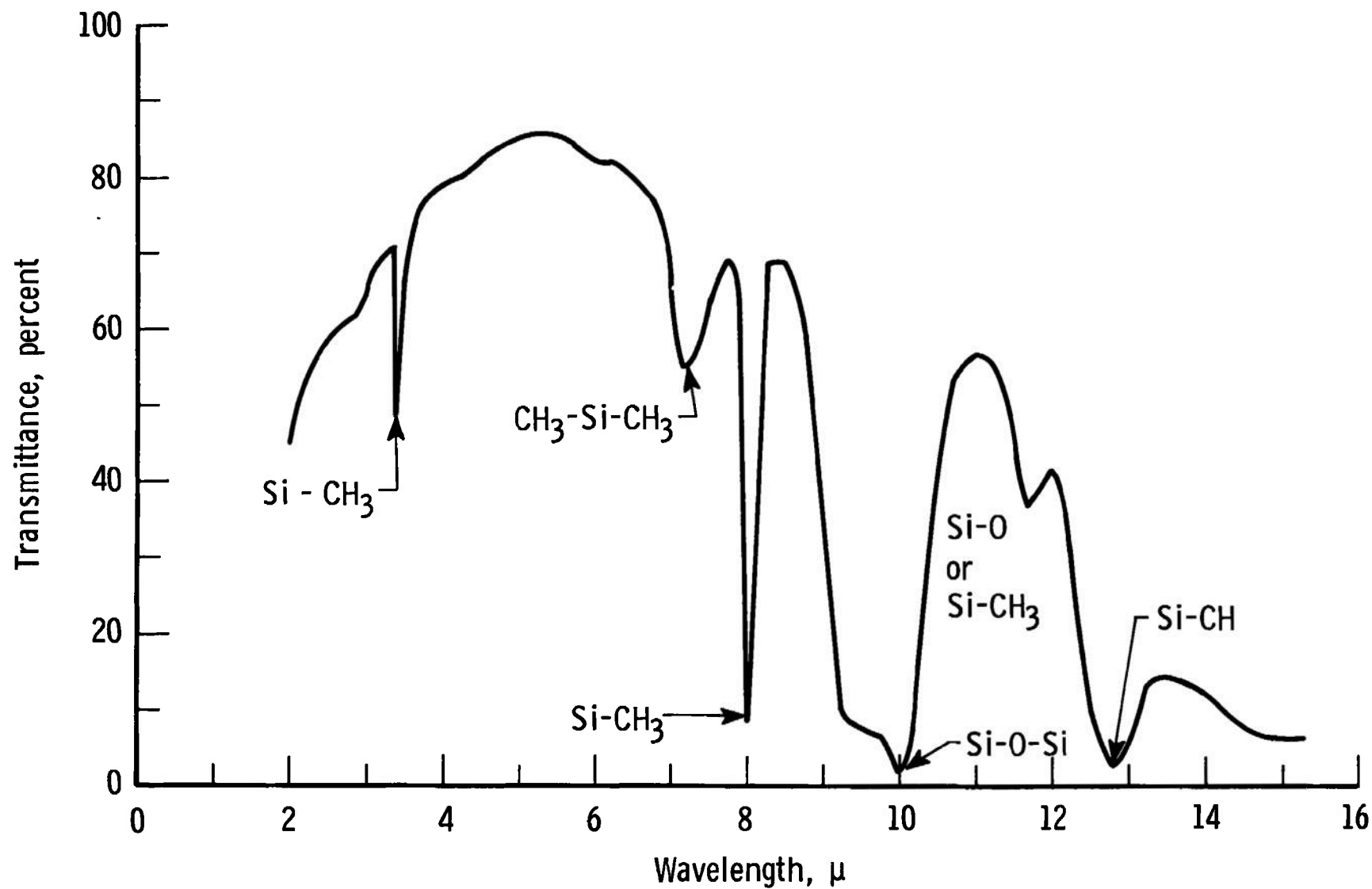


Fig. 16 Infrared Spectra of a Nonirradiated Sample

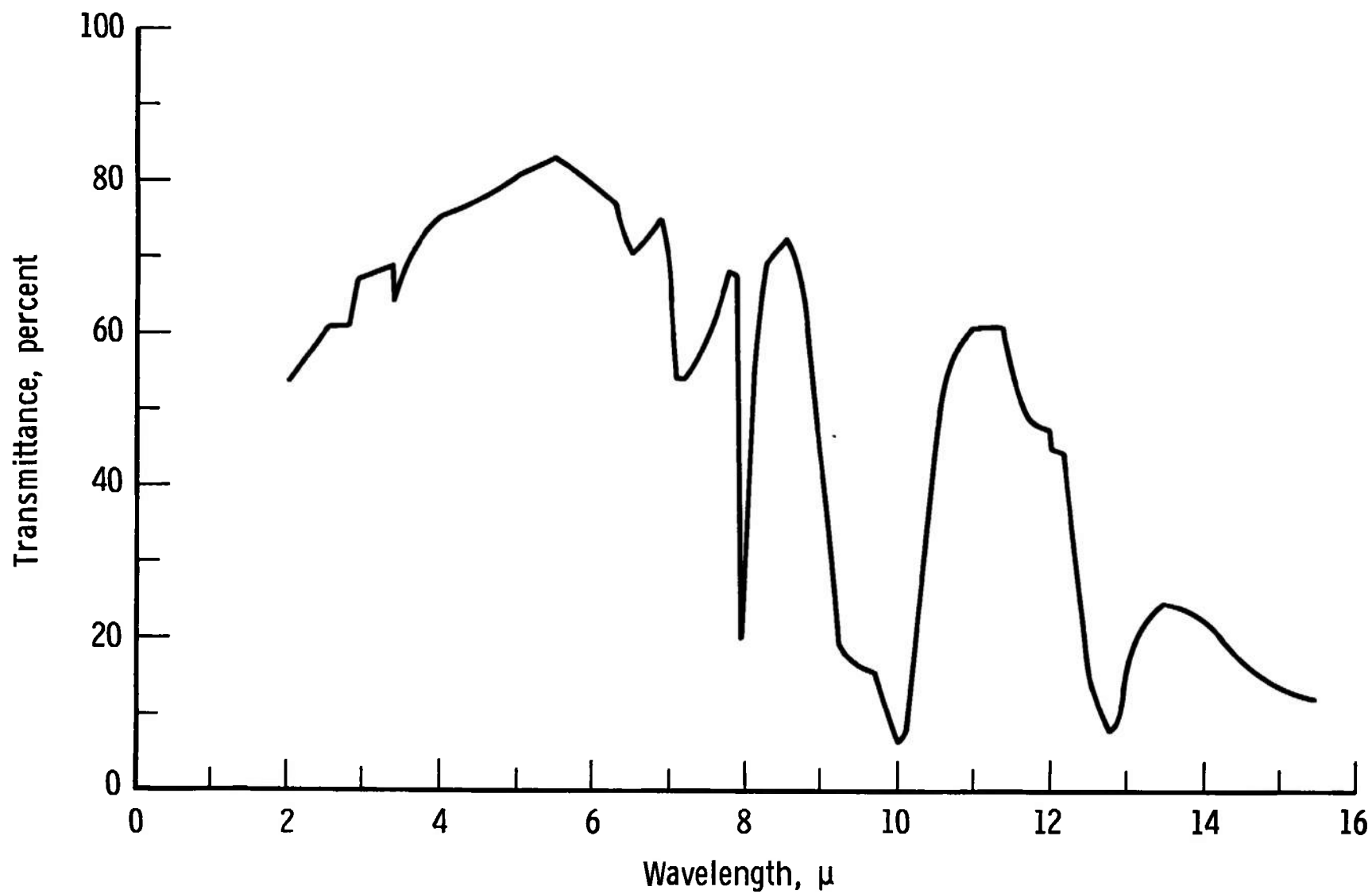


Fig. 17 Infrared Spectra of Electron Irradiated (Low Rate) Sample

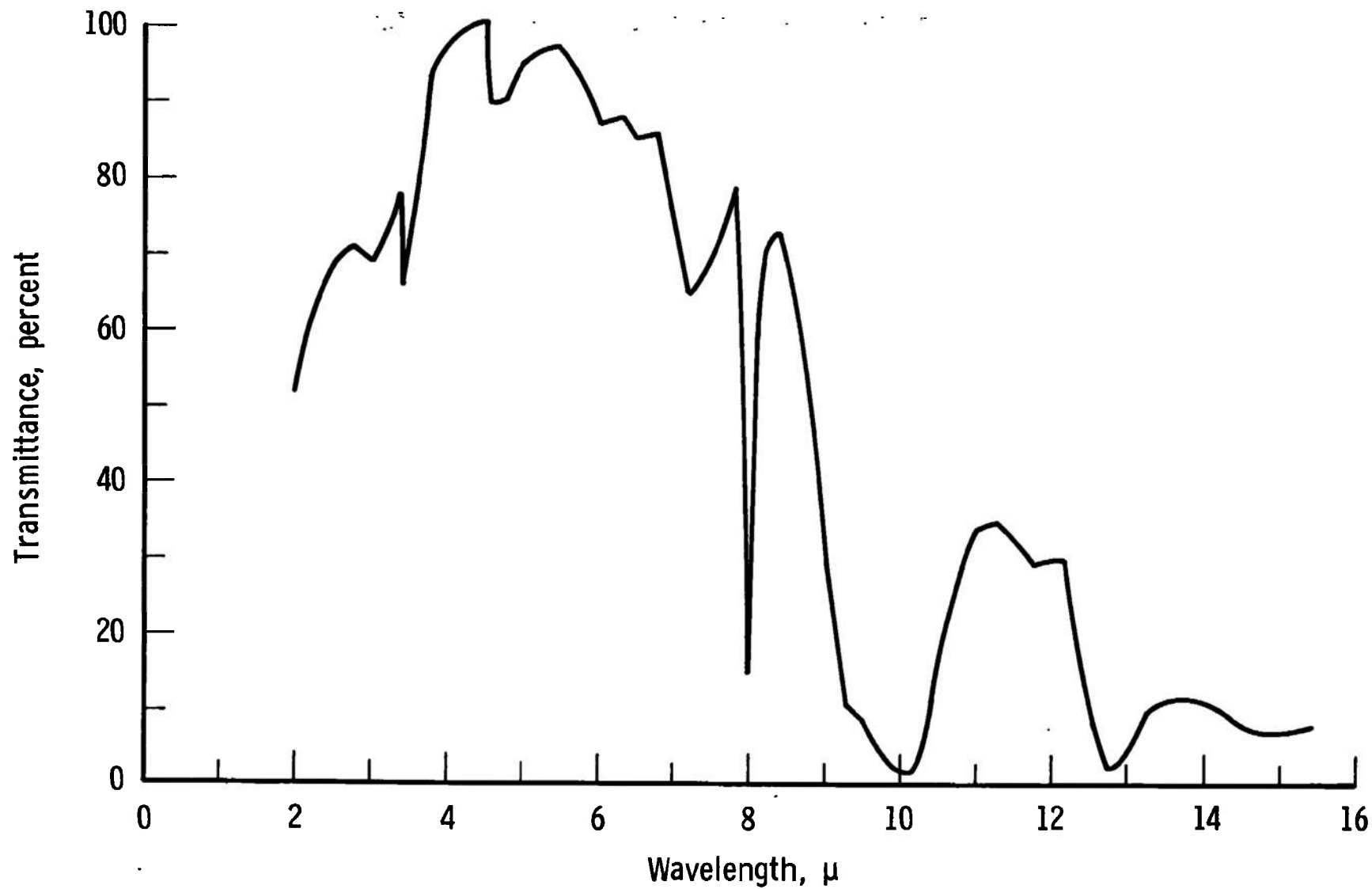


Fig. 18 Infrared Spectra of Proton Irradiated Sample

44

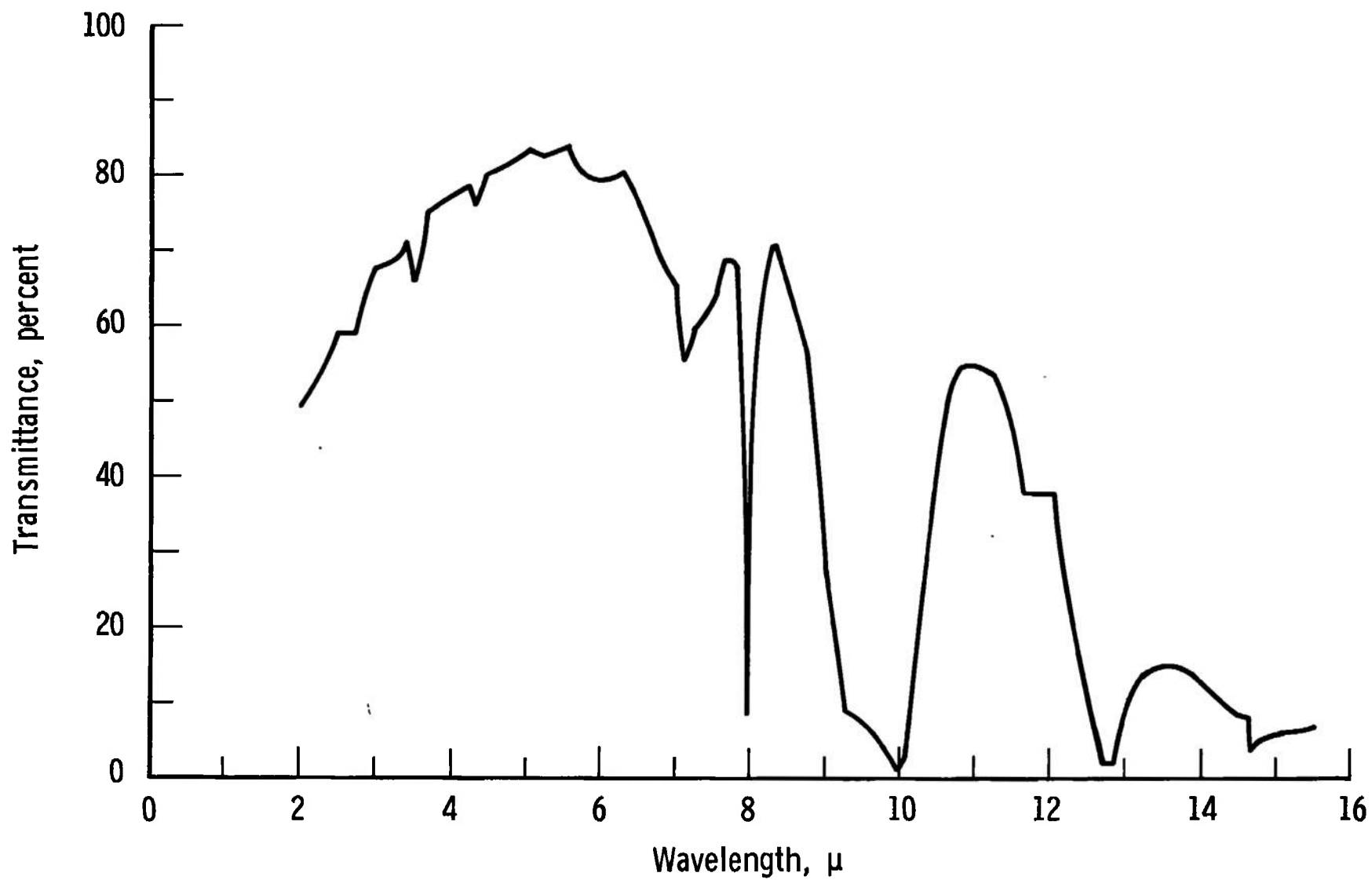


Fig. 19 Infrared Spectra of Electron Irradiated (High Rate) Sample

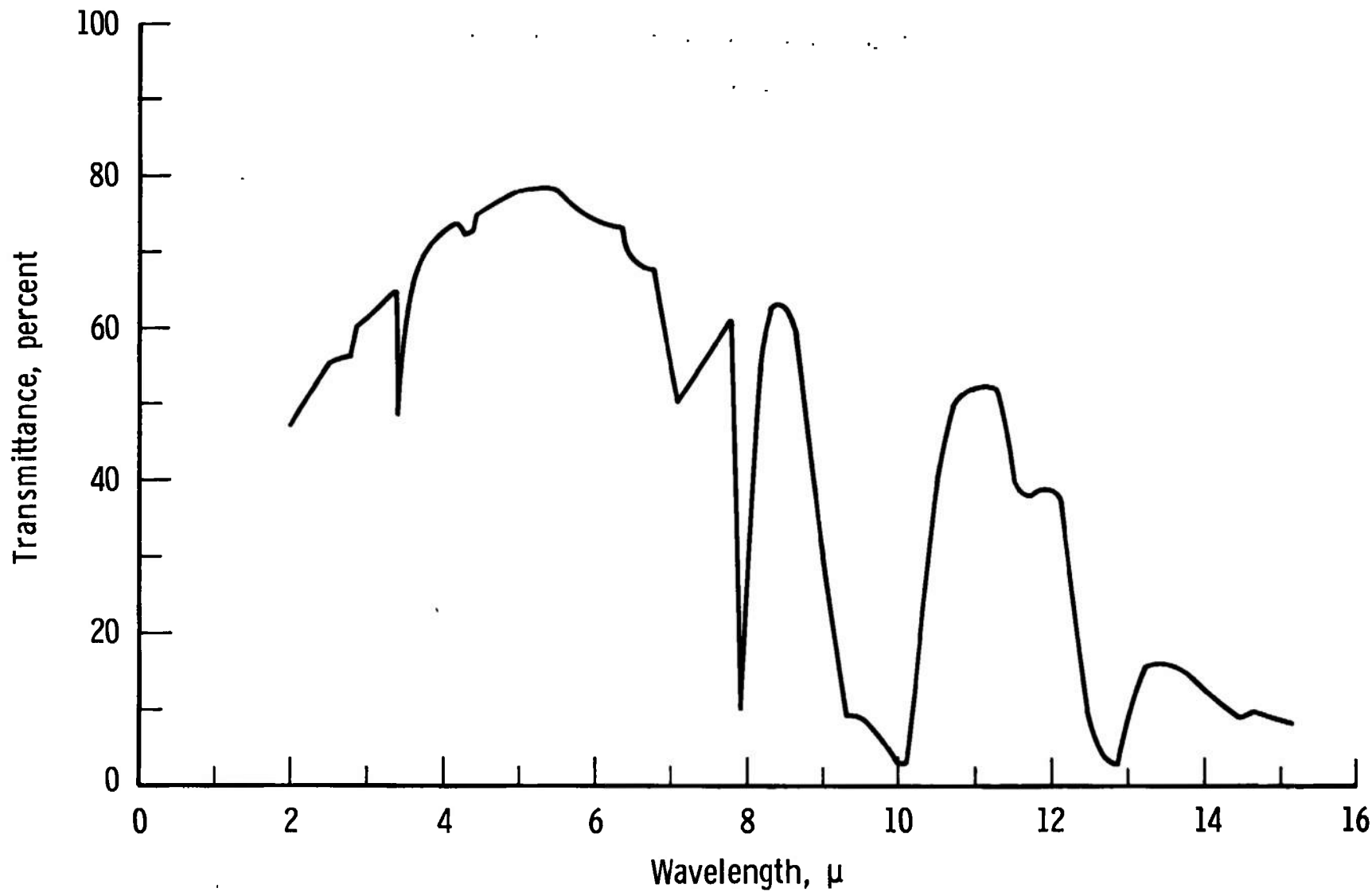


Fig. 20 Infrared Spectra of Electromagnetic Radiation Sample

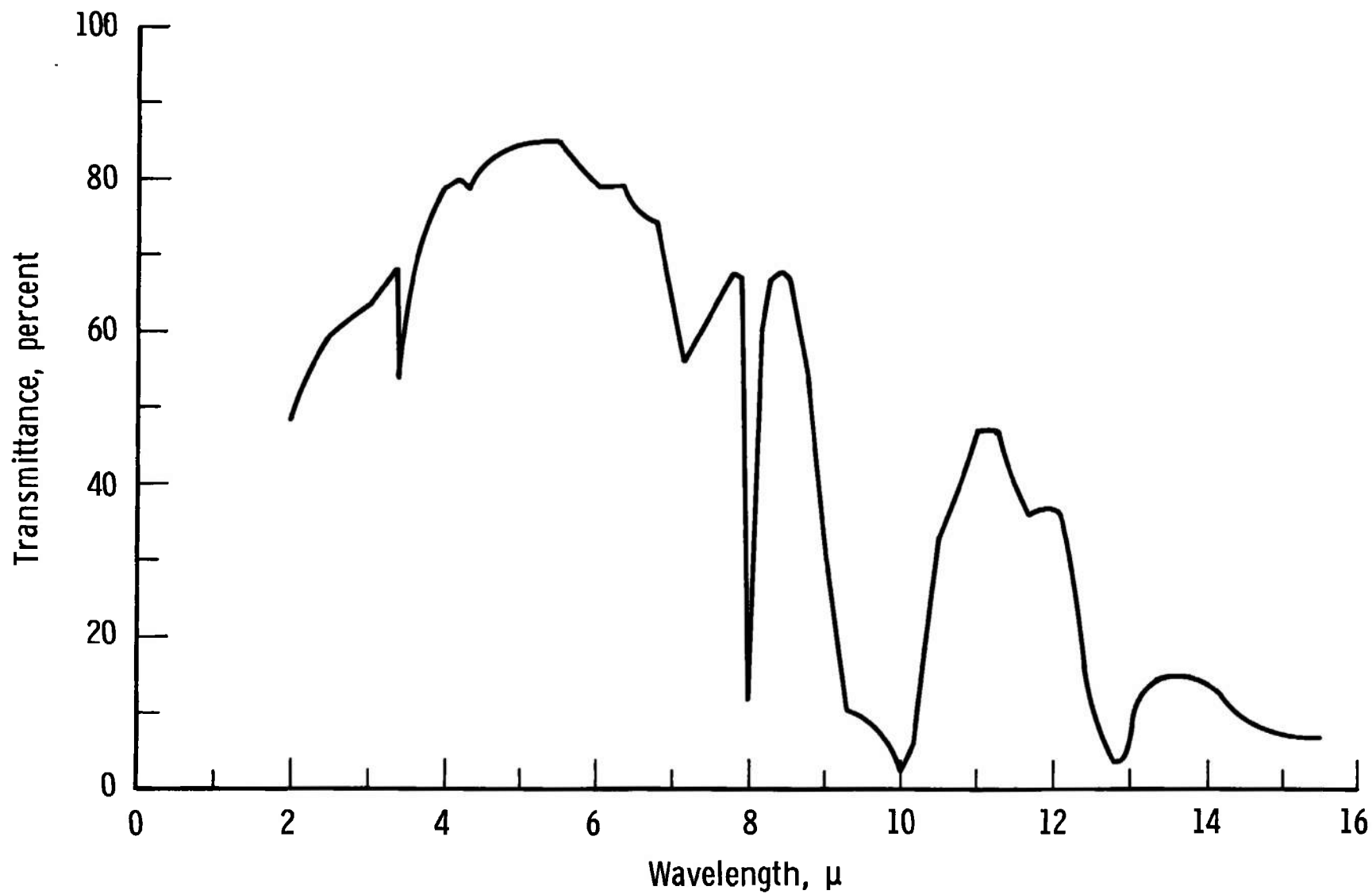
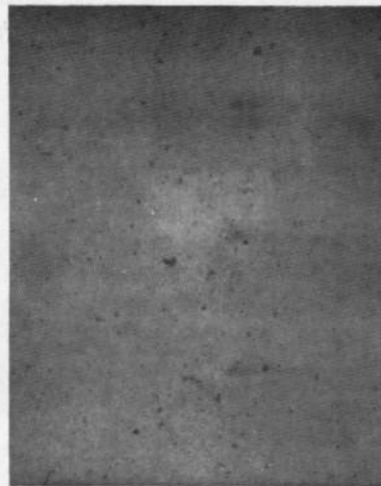


Fig. 21 Infrared Spectra of Combined Environment Sample



a. No Exposure (100x)



b. Electromagnetic Radiation and Vacuum (100x)



c. Low Rate Electrons and Vacuum (100x)



d. High Rate Electrons and Vacuum (100x)

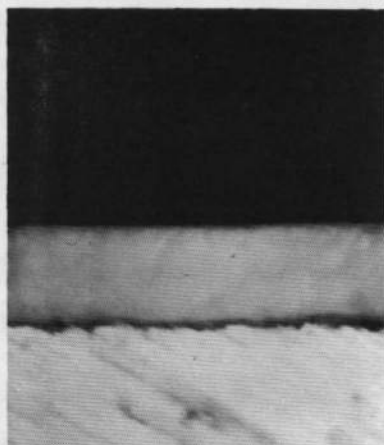


e. Protons and Vacuum (100x)

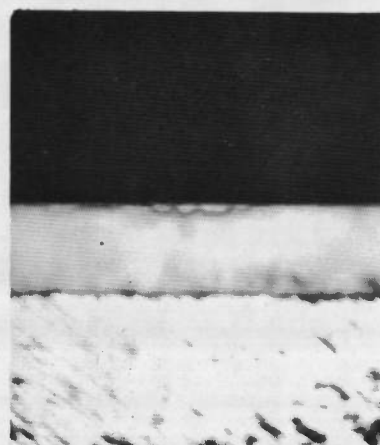


f. Protons, Electrons, Electromagnetic Radiation and Vacuum (100x)

Fig. 22 Photomicrograph of the Surface of the Test Samples



a. No Exposure (200x)



b. Electramagnetic Radiation and Vacuum (200x)



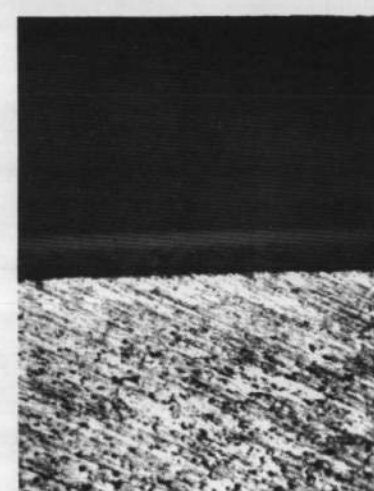
c. Low Rate Electron and Vacuum (100x)



d. High Rate Electrans and Vacuum (100x)



f. Protans, Electrans, Electramagnetic Radiation, and Vacuum (100x)



e. Pratons and Vacuum (100x)

Fig. 23 Photamicrograph of the Crass Section of the Test Samples

**TABLE I**  
**COMBINED ENVIRONMENT EFFECTS EVALUATION AS DETERMINED BY**  
**CHANGES IN THE SPECTRAL REFLECTANCE OF COATING**

Wavelength, $\mu$	0.5	1.0	1.5	2.0	2.4
Environment	Change in Spectral Reflectance, percent				
Vacuum	0	0	0	0	0
Electromagnetic Radiation and Vacuum	-1	-2	-1	0	+1
Electrons and Vacuum	-28	-50	-50	-41	-27
Protons and Vacuum	-18	-11	-9	-4	+2
Sum of Individual Changes	-47	-63	-60	-45	-24
Combined Environment	-40	-43	-38	-24	-13
Combined Environment Difference, percent	-7	-20	-22	-21	-11

**TABLE II**  
**COMBINED ENVIRONMENT EFFECTS EVALUATION AS DETERMINED BY**  
**INTEGRATED SOLAR REFLECTANCE AND ABSORPTANCE**

Environment	Change in Integrated Solar Reflectance, percent	Change in Integrated Solar Absorptance, percent
Vacuum	0	0
Electromagnetic Radiation and Vacuum	-2	+3
Electrons and Vacuum	-39	+89
Protons and Vacuum	-13	+28
Sum of Individual Changes	-54	+120
Combined Environment	-38	+84
Combined Environment Difference, percent	-16	-36

**TABLE III**  
**ELECTRON RATE EFFECT SUMMARY**

Time Integrated Flux, electrons/cm <sup>2</sup>	Change in Integrated Solar Absorptance, percent		Difference, percent
	6.3 x 10 <sup>10</sup> electrons/cm <sup>2</sup> /sec	6.3 x 10 <sup>11</sup> electrons/cm <sup>2</sup> /sec	
5.67 x 10 <sup>14</sup>	12.3	18.7	6.4
1.06 x 10 <sup>15</sup>	18.1	24.0	5.9
1.63 x 10 <sup>15</sup>	21.7	27.3	5.6

UNCLASSIFIED

Security Classification

## DOCUMENT CONTROL DATA - R &amp; D

(Security classification of title, body of abstract and indexing annotation must be entered when the overall report is classified)

## 1. ORIGINATING ACTIVITY (Corporate author)

Arnold Engineering Development Center  
 ARO, Inc., Operating Contractor  
 Arnold Air Force Station, Tennessee 37389

## 2a. REPORT SECURITY CLASSIFICATION

UNCLASSIFIED

## 2b. GROUP

N/A

## 3. REPORT TITLE

INITIAL RESULTS FROM A COMBINED SPACE ENVIRONMENT EFFECTS CHAMBER

## 4. DESCRIPTIVE NOTES (Type of report and inclusive dates)

Final Report

## 5. AUTHOR(S) (First name, middle initial, last name)

W. G. Kirby and C. N. Warren, ARO, Inc.

## 6. REPORT DATE

October 1968

## 7a. TOTAL NO. OF PAGES

57

## 7b. NO. OF REFS

16

## 8a. CONTRACT OR GRANT NO.

F40600-69-C-0001

## 9a. ORIGINATOR'S REPORT NUMBER(S)

AEDC-TR-68-139

## 9b. OTHER REPORT NO(S) (Any other numbers that may be assigned this report)

N/A

## 10. DISTRIBUTION STATEMENT

This document has been approved for public release and sale;  
 its distribution is unlimited.

## 11. SUPPLEMENTARY NOTES

Available in DDC.

## 12. SPONSORING MILITARY ACTIVITY

Arnold Engineering Development  
 Center (AETS), Arnold Air Force  
 Station, Tennessee 37389

## 13. ABSTRACT

A combined environment research chamber has been designed and built to provide the capability of irradiating test samples with protons, electrons, and electromagnetic radiation, individually, sequentially, or simultaneously, in a clean high vacuum utilizing a multisample holder and an in situ spectral reflectance measurement technique. The chamber performance was evaluated on the basis of a combined environment test conducted on a titanium dioxide-methyl silicone thermal control coating and was found to be completely satisfactory. In the combined environment experiment, samples of the thermal control coating were exposed individually to vacuum, protons, electrons, electromagnetic radiation, and to all of these constituents simultaneously. No synergistic effects were noted. However, a combined environment interaction was noted wherein the sum of the individual effects was greater than that obtained in the simultaneous exposure.

## KEY WORDS

## LINK A

## LINK B

## LINK C

ROLE

WT

ROLE

WT

ROLE

WT

environmental testing

space simulation

combined effects

test facilities

1. Combined space environment effects Chamber
2. " environment chamber
2. Space chamber - A&E
4. " " " " Performance

17-3